NOTE TO USERS

uOttawa

L'Université canadienne
Canada's university

FACULTÉ DES ÉTUDES SUPÉRIEURES ET POSTOCTORALES

uOttawa

L'Université canadienne
Canada's university

FACULTY OF GRADUATE AND POSDOCTORAL STUDIES

Stephan Chan-Taw
AUTEUR DE LA THÈSE / AUTHOR OF THESIS

M.A.Sc. (Electrical Engineering)
GRADE / DEGREE

School of Information Technology and Engineering
FACULTÉ, ÉCOLE, DÉPARTEMENT / FACULTY, SCHOOL, DEPARTMENT

Performance of Linear Detectors Using Partial Decision Techniques in CDMA Systems with Multiple Antenna

TITRE DE LA THÈSE / TITLE OF THESIS

Claude D'Amours
DIRECTEUR (DIRECTRICE) DE LA THÈSE / THESIS SUPERVISOR

Tricia Willink
CO-DIRECTEUR (CO-DIRECTRICE) DE LA THÈSE / THESIS CO-SUPERVISOR

EXAMINATEURS (EXAMINATRICES) DE LA THÈSE / THESIS EXAMINERS

Tyseer Aboulnasr

Florence Danilo-Lemoine

Gary W. Slater
LE DOYEN DE LA FACULTÉ DES ÉTUDES SUPÉRIEURES ET POSTDOCTORALES /
DEAN OF THE FACULTY OF GRADUATE AND POSTDOCORAL STUDIES

Performance of Linear Detectors Using Partial Decision Techniques in CDMA Systems with Multiple Antenna

by

Stephan Chan-Taw

Thesis submitted to the
Faculty of Graduate and Postdoctoral Studies
In partial fulfillment of the requirements
For the M.A.Sc. degree in
Electrical and Computer Engineering

School of Information Technology and Engineering
Faculty of Engineering
University of Ottawa

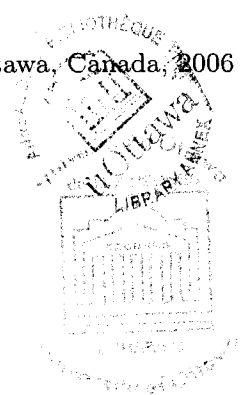

Your file Votre référence
ISBN: 978-0-494-41789-8
Our file Notre référence
ISBN: 978-0-494-41789-8

Abstract

Partial decision variables exploit the code diversity available in a code division multiple access system by detecting the received signal over different portions of the signaling interval to produce multiple decision intervals. Decision variables can then be weighted using adaptive filtering techniques, improving signal to interference plus noise ratio. In this thesis, we integrate the partial decision variable technique with multiple antennas to further improve performance by exploiting spatial diversity without greatly increasing the complexity of the system. Specifically, we will demonstrate the use of the partial decision variable technique through simulated and measured channel data for different configurations of single and multiple antenna system with least mean square weighting. Further, a multiuser detection technique using partial decision variables is developed for space-code division multiple access which significantly reduces the effects of multi-access and self interference to provide good performance with low incremental complexity. Throughout this thesis we will show using simulations and discussion that the use of multiple partial decision variables provide better BER performance over single decision variable systems at higher signal to noise ratios. Overall the use of multiple PDV with properly chosen least mean square step sizes, can provide additional gain with relatively low increase in complexity.

Acknowledgements

First and foremost, I would like to express my deepest gratitude to my supervisor Claude D'Amours for giving a student who was initially lost and confused, a direction in life. Although I have only worked with Dr. D'Amours for 2 years, I feel that he has treated and respected me as a part of his family. As I put together the final pieces of my thesis together, I have realized that most of my work could not have been completed without his guidance and continual support. The knowledge that I have gained from him, I will cherish throughout the years.

I am grateful for the financial support provided by Defence Research & Development Canada (DRDC) through the Defence Communication Program at the Communication Research Centre (CRC). I am also grateful to CRC for the use of facilities and equipment throughout my research. At the CRC, I would first like to extend my gratitude to Dr. Tricia Willink who supervised me throughout my thesis research at the CRC. During my time at CRC, she continually encouraged and supported me in the completion of my thesis, always reminding me always to aim higher than what you'd expect from yourself. With her extensive knowledge in wireless communications, she has assisted me numerous times when questions arised. Secondly, I would like to give a special thanks Geoff Colman for all his support over the past year, without his knowledge and guidance I would not have accomplished this thesis. Finally, I would like to thank all of my colleagues Chris Squires, Jeffery Wells, Luis Gurrieri and Garfield Downes for all their input on a wide variety of topics. Not until now do I realize the vast knowledge within my grasp.

My sincere thanks and appreciation also to all my family and friends for continually motivating me and showing me that there is light at the end of the tunnel. Without their support, my focus would have dwindled away from my goal to complete my thesis. As a special thanks I would like to present it to a person who has waited for me for 7 years. Thank you Cindy for all your patience and understanding. I'm coming home soon.

When I look back at these two years, it seemed like the journey was a long and difficult road. But when I think about what everyone has done for me, the road traveled seemed to an enjoyable one.

Contents

List of Figures

List of Acronyms

AWGN	:	Additive White Gaussian Noise
BER	:	Bit Error Rate
BPSK	:	Binary Phase Shift Keying
CDMA	:	Code Division Multiple Access
DF	:	Decision Feedback
DMI	:	Direct Matrix Inversion
DS-CDMA	:	Direct Sequence Code Division Multiple Access
FDMA	:	Frequency Division Multiple Access
FFT	:	Fast Fourier Transform
IFFT	:	Inverse Fast Fourier Transform
ISI	:	Inter Symbol Interference
LCMLL	:	Linearly Constrained Maximum Likelihood Linear
LCMV	:	Linearly Constrained Minimum Variance
LMS	:	Least Mean Squares
LOS	:	Line Of Sight
MAI	:	Multiple Access Interference
MFB	:	Matched Filter Bank
MIMO	:	Multiple Input Multiple Output
ML	:	Maximum Likelihood
MLS	:	Maximum Likelihood Sequence
MMSE	:	Minimum Mean Square Error
MUD	:	Multiuser Detection
PDV	:	Partial Decision Variable
PIC	:	Parallel Interference Cancellation
PSD	:	Power Spectrum Density
PSIR	:	Pilot Symbol Insertion Rate

RLS	:	Recursive Least Square
SCDMA	:	Space-Code Division Multiple Access
SIC	:	Successive Interference Cancellation
SINR	:	Signal to Interference and Noise Ratio
SIMO	:	Single Input Multiple Output
SISO	:	Single Input Single Output
SM	:	Spatial Multiplexing
SNR	:	Signal to Noise Ratio
SS	:	Spreading Sequence
SF	:	Spreading Factor
STBC	:	Space-Time Block Codes
ST-MUD	:	Space-Time Multiuser Detector
TDMA	:	Time Division Multiple Access
WSS	:	Wide Sense Stationary

List of Symbols

$\mathbf{A}$	:	Correlation matrix
b_n	:	Information bit of the desired user
b_{l_b}	:	Desired users information bit at the desired time interval
$\hat{b}_n$	:	Estimated Data bit
B_c	:	Coherence bandwidth
c_n	:	Code factor for symbols of interest
d	:	Desired signal
$\mathbf{D}$	:	Diagonal of complex channel gain
$\mathbf{D}_r$	:	Diagonal amplitude matrix
e	:	Estimation error
η	:	Fraction of channel symbols to are bits
η_n	:	Desired users matched filter response for noise
f_c	:	Carrier frequency
f_d	:	Doppler frequency
G_a	:	Azimuthal Gain
G_w	:	Noise whitening filter
$\mathbf{G}$	:	Coding block
$\mathbf{G}_i$	:	Nulling Matrix
$\mathbf{G}_n$	:	Coding block for desired user
h	:	Channel coefficients
$\mathbf{h}$	:	Channel gain vector
$\mathbf{I}$	:	Identity Matrix
k	:	Desired chip sample
K	:	spreading factor
l_b	:	Desired but for transmitted by user
L_b	:	Length of desired users information bits

μ : LMS step size
M : The number of received signal on one antenna
n : Desired user
N : Number of users
N_r : Number of receive antennas
N_t : Number of transmit antennas
N_o : Noise spectral density
$\mathbf{n}$: Noise vector
$\mathbf{p}$: Implicit channel response
$r(t)$: Received signal
ρ : Cross correlation between signals
$\mathbf{r}$: Received vector
$\mathbf{R}$: Auto correlation of received signal
s : Number of information bits
σ_n^2 : Noise variance
$\mathbf{s}$: Transmitted signal
T : Symbol Period
T_c : Delay Spread
T_l : Training length
T_s : Number of time slots
t_s : Desired time slot
$u(t)$: Decorrelated signal
$\mathbf{u}$: Decision variable vector
v : Velocity
W : Signal bandwidth
W_{mmse} : Weighting for MMSE
$\mathbf{w}_{opt}$: Optimum weighting vector
$\mathbf{w}_{DMI}$: Optimized DMI weighting vector
$\mathbf{w}$: LMS weights
X_s : Number of symbols sent
x : Desired subinterval
X : Number of subintervals
y : Decision variable

Chapter 1

Introduction

1.1 Motivation

With the rapid growth of wireless communication, cellular networks have been increasing at a much faster rate than wireline telephone networks [1]. The main driving force behind this growth is the portability and reliability that wireless services can provide to users as a source of communication. Adding to this growth is the increased functionality of wireless devices. Not only can these devices support voice, multimedia content has now become the norm in personal communication. To maintain this steady growth, improvements are needed to increase capacity in current networks. One method to accomplish this is by improving bit-error rate (BER) performances of multiple access techniques allowing more information to be transferred reliably.

In frequency division multiple access (FDMA), users transmit information over non-overlapping segments of the available bandwidth while in time division multiple access (TDMA), users utilize the entire allocated bandwidth while subdividing it into time slots, where each slot only one user is allowed to transmit or receive. Unlike FDMA and TDMA, code division multiple access (CDMA) users can transmit simultaneously while occupying the entire available band of frequencies for transmission. A commonly-used form of CDMA is direct sequence code division multiple access (DS-CDMA) [2] where the data signal is directly multiplied by a spreading sequence. In a DS-CDMA system shown in Figure 1.1 each user's data stream is multiplied by a unique spreading sequence (SS), that repeats every bit interval. After transmission of the signal, the receiver detects a signal composed of a sum of multiple signals that has been multiplied by their individual spreading sequence plus noise. With knowledge of the desired user's SS, the receiver uses coherent demodulation to

despread the received signal. To be able to perform this operation, the receiver not only needs to know the desired user's SS but also synchronization is needed between the generated SS and the received signal.

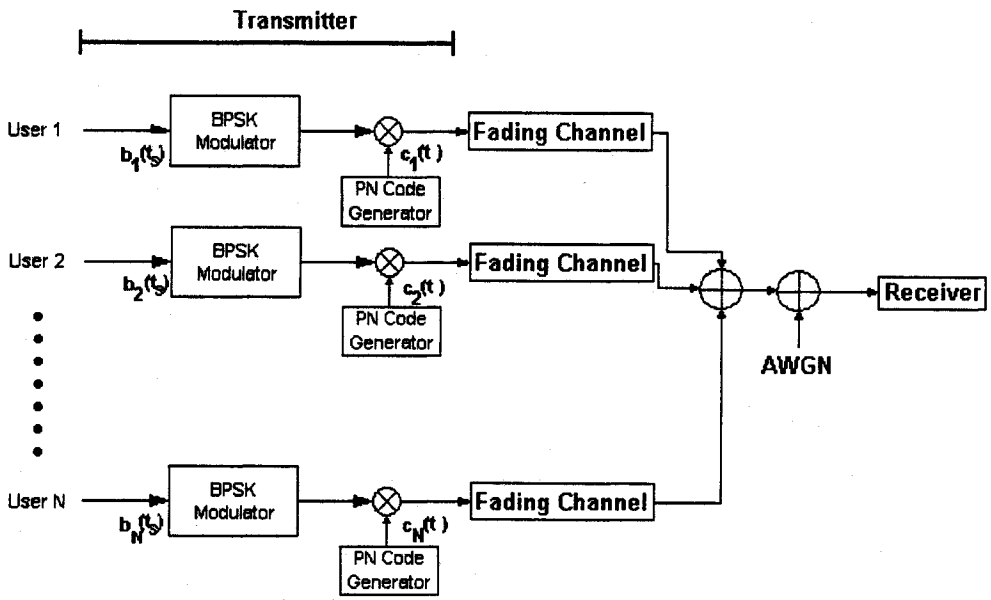

Figure 1.1: DS-CDMA system model.

In this thesis our main focus is on CDMA systems. The advantages of using CDMA include the following:

- Unlike TDMA and FDMA systems, CDMA systems have a soft capacity limit. Instead of having a limit on the number of users a system can handle, CDMA allows for a increase in the number of users by decreasing its performance.
- Each bit of data is CDMA system are identified by a spreading sequence that only the transmitter and receiver knows, preventing other users from receiving your data.
- Current 3G technologies which include WCDMA, CDMA2000, and TD-SCDMA, focuses on providing the ability to transfer voice and multimedia (email, messaging, and downloading) information, use CDMA as their multiple access scheme.

In an ideal DS-CDMA system all spreading waveforms are orthogonal, allowing for simultaneously transmitted signals to be detected without interference. In a synchronous mobile

system, mobile users are not situated in the same location, causing DS-CDMA signal to experience multipath fading. Due to this phenomenon, signals from different users arrive at the receiver with different time delays, resulting in de-orthogonalized SSs, creating MAI. In asynchronous mobile systems, in addition to multipath fading, different time delays for transmission are present, which we have no control over, thus having no control over the cross-correlation between interfering users. This is a major concern in DS-CDMA systems, because of the limiting characteristics of multiple access interference (MAI), overall performance of the system can degrade. MAI refers to interference caused by simultaneous usage of the channel by multiple users. While the MAI between different pairs of users is relatively small, MAI increases as the number of users increases.

In a conventional system, each user is detected independently and MAI is considered as thermal noise. Although MAI might be negligible when dealing with a small number of users, MAI increases as the number of users increases, resulting in BERs that are much greater than in a single user system. To improve capacity performance to facilitate voice and multimedia communication, systems have to reduce MAI to allow more users to access the channel with reliable BER performance. In order to reduce the effect of interference, detector designs need to take the effect of interfering signals into account. Current research examines the use of multiuser detection (MUD) to address the problem of MAI. Different MUD designs are usually receiver based and require tradeoffs between complexity and performance. While complex systems provide better performance, costs for implementation may deter industry from adopting multiuser techniques.

This brings us to the main focus of this thesis, to design a system that is low in complexity while providing improved BER performance compared to conventional CDMA systems.

1.2 Objective of this Thesis

The main purpose of this thesis is to develop and evaluate a low complexity multiuser system that can be easily implemented. To try and reduce MAI in DS-CDMA systems, we propose using a simple receiver based on the partial decision variable (PDV) technique. The technique was presented in [3], demonstrating the use of adaptive filtering along with decision feedback for determining weights between the output of the matched filter and the multiuser detector. Results showed that given a system with three users and a single receive antenna overall BER performance can be improved with little increase in computational complexity. This thesis will extend the work done in [3] to the case of a wireless communication system where single and multiple transmit/receive antennas are used. The BER performance of our

proposed system is determined by simulation in ideal channels (slow frequency nonselective Rayleigh fading channels) and using measured channel data. For the ideal case, fading gains encountered on each transmit-receive antenna pair are assumed to be independent identically distributed (i.i.d.) complex Gaussian random variables. The efficiency of this system will be explored by evaluating the BER performance for different system parameters. In summary, our system will show the following:

1. PDV uses adaptive weights to improve the received signal to interference plus noise ratio (SINR), MAI reduction can be achieved without knowledge of the interfering user's spreading sequences.

2. By exploiting the MAI reducing properties, we will reduce MAI using both multi-antenna receiver/transmitters and the PDV technique.

3. Using multi-antenna receivers require channel gain knowledge for effective reconstruction of signals. Our system preforms PDV weighting and channel gain corrections in the same process.

4. Using PDVs decreases complexity compared to existing MUDs with multiple antennas without greatly reducing BER performance.

1.3 Outline of Thesis

This thesis is organized as follows:

Chapter 2 gives general background on previously designed MUDs, this is followed by a review on current research done in the area of MUDs and multiple antenna systems.

Chapter 3 presents general system parameters in conjunction with the proposed technique which are used throughout this thesis, followed by descriptions of channel characteristics, describing why and how they are implemented.

Chapter 4 focuses on adaptive algorithms, describing optimal weighting and suboptimal weighting for combining signals. The use of adaptive algorithms plays an important role in optimizing PDV detection, which will also be described in this chapter, combining different PDVs together to form a better decision variable.

In chapter 5, the modified PDV technique is discussed in more detail, and the performance of this technique is demonstrated and compared through simulations to the conventional receiver. By extending this technique to multiple receive antennas and varying specific parameters, we will discuss and illustrate our results through simulated and measured channel data with examples.

In chapter 6, we further extend partial spreading sequences to include transmit diversity. System performance is demonstrated through simulated and measured channel data for different configurations of single and multiple antenna transmitters/receivers. The extension of the technique to provide adaptive data rates by varying specific parameters will also be discussed and illustrated with examples.

Finally, chapter 7 summarizes work accomplished and results obtained throughout this thesis and recommendations are made for future research.

Chapter 2

Background

2.1 Background on DS-CDMA Systems and Multiuser Detectors

The previous chapter briefly outlined the main objectives of this thesis. In this chapter we will first look at the conventional detector, this will be followed with discussion on the optimal multiuser detector as well as common sub-optimal multiuser detectors for DS-CDMA systems.

2.1.1 Received Signal System Model

In this thesis, we consider a narrowband synchronous N user DS-CDMA system employing binary phase shift keying (BPSK) modulation. The baseband model of a transmitted signal for user n transmitting on K chip intervals (In other words, each symbol is divided into K chip intervals or a spreading factor of K) is given by:

$$s_n(k) = b_n(t_s)c_n(k) \quad 0 \leq k \leq K-1 \tag{2.1}$$

where

$b_n(t_s)$	=	data bit in symbol interval of interest t_s
c_n	=	spreading sequence in symbol interval of interest
n	=	desired user
k	=	chip sample index
K	=	spreading factor.

The received signal $r(k)$ is the sum of all users' data multiplied by their respective spreading sequences and channel coefficients h_n plus a Gaussian noise component of zero mean and variance σ_n^2:

$$r(k) = \sum_{j=1}^{N} h_j s_j(k) + n(k) \tag{2.2}$$

2.1.2 Conventional Detector

In the conventional detector shown in Figure 2.1, the received signal described in equation (2.2) is received by a bank of N correlators. To demodulate the signal for the desired user, the received signal is correlated with the desired spreading sequence, this process is also known as matched filtering [4], to produce a decision for bit t_s as:

$$\begin{aligned} u_n &= \sum_{k=0}^{K-1} r(k)c_n(k) \\ &= \sum_{j=1}^{N}\sum_{k=0}^{K-1} h_j b_j(t_s)c_j(k)c_n(k) + \sum_{k=0}^{K-1} n(k)c_n(k) \\ &= \sum_{j=1}^{N} h_j b_j(t_s) \sum_{k=0}^{K-1} c_j(k)c_n(k) + \nu_n \\ &= \sum_{j=1}^{N} h_j b_j(t_s) K\rho_{nj} + \nu_n \\ &= h_n b_n(t_s)K + \sum_{j=1, j\neq n}^{N} h_j b_j(t_s) K\rho_{nj} + \nu_n \end{aligned} \tag{2.3}$$

where the first term in (2.3) represents the desired user's signal, the second term represents the MAI and ρ_{nj} is the cross correlation between the spreading waveforms of users n and j given by:

$$\rho_{nj} = \frac{1}{K}\sum_{k=0}^{K-1} c_n(k)c_j(k) \tag{2.4}$$

and the third term ν_n is the matched filter's response to input white Gaussian noise. From equation (2.3), if on average ρ_{nj} is very small (i.e. $|\rho_{nj}| \ll 1$), the receiver is able to detect the transmitted data bit with all other interfering information symbols appearing as noise.

The expression in (2.3) can also be written in matrix form as:

$$\begin{bmatrix} u_1 \\ u_2 \\ \vdots \\ u_N \end{bmatrix} = K \begin{bmatrix} 1 & \rho_{12} & \dots & \rho_{1N} \\ \rho_{12} & 1 & \dots & \rho_{2N} \\ \vdots & \vdots & \ddots & \vdots \\ \rho_{1N} & \rho_{2N} & \dots & 1 \end{bmatrix} \cdot \begin{bmatrix} h_1 & 0 & \dots & 0 \\ 0 & h_2 & \dots & 0 \\ \vdots & \vdots & \ddots & \vdots \\ 0 & 0 & \dots & h_N \end{bmatrix} \cdot \begin{bmatrix} b_1 \\ b_2 \\ \vdots \\ b_N \end{bmatrix} + \mathbf{n} \tag{2.5}$$

or compactly as $\mathbf{u} = K\mathbf{ADb} + \mathbf{n}$ where $\mathbf{A}$ is defined as the correlation matrix, $\mathbf{D}$ is the diagonal complex channel gain matrix and $\mathbf{n}$ is the complex Gaussian noise vector.

When using conventional detection the receiver requires no prior knowledge of the interfering users' signals. From Figure 2.1 the conventional detector uses each individual branch to detect each desired user's signal without regard to any interference caused by other users. To reduce the effect of MAI and increase the reliability of DS-CDMA systems, different solutions can be considered. These include: increasing SNR, reducing cross-correlation between spreading sequences, or receiver designs.

If we increase the SNR, the transmitting user increases its transmission power. This will in turn cause the decision signal for other users to have increased MAI, forcing them to compensate by increase their own transmit power and does not increase performance. When using orthogonal spreading sequences MAI is reduced to zero. However, as discussed before, time delays de-orthogonalize the SSs, creating MAI. To reduce, MAI different receivers can be designed such as the optimal detector and several other sub-optimal detectors discussed below.

2.1.3 Multiuser Maximum-Likelihood Sequence (MLS) Detector

In 1986 an optimal multiuser detection was developed by S. Verdu [5] which offers significant improvements over the conventional detector. By implementing a Viterbi algorithm after the conventional detector, the maximum likelihood (ML) detector can only be solved by an exhaustive search of all possible outcomes of the received signals. This method, illustrated in Figure 2.2, although optimum, will require 2^{NK} calculations to find the maximum likelihood sequence for a N-user synchronous system over a K chip signaling interval. This detector can be implemented by utilizing a bank of matched filters followed by a detector based on the Viterbi algorithm. The computational complexity of this method is exponentially proportional to the number of users which does not allow for systems with a large number of simultaneous users. Since a large performance gap exists between conventional and optimal detection, over the years many suboptimal detectors have been developed to combat MAI

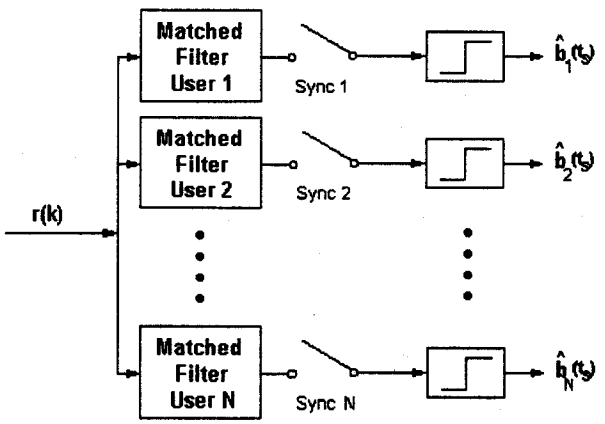

Figure 2.1: Conventional detector.

while maintaining lower complexity than Verdu's detector [6–9]. However, when using sub-optimal detectors design trade offs are often needed. This section reviews several important detectors previously designed, taking different trade offs into account.

2.1.4 Suboptimal Linear Detectors

In linear MUD a linear transformation is applied to the soft (non-quantized) outputs of the conventional detector $\mathbf{u}$ to produce a new decision variable reducing the amount of MAI seen by each user. Common linear detectors include the decorrelating and minimum mean square error (MMSE) detectors.

Decorrelating Detector

The decorrelating detector in [7] is shown to be able to eliminate MAI completely if the spreading waveforms of the users are linearly independent. Considering the received signal from equation (2.5) then:

$$\mathbf{u} = K\mathbf{A}\mathbf{D}_r\mathbf{b} + \mathbf{n} \tag{2.6}$$

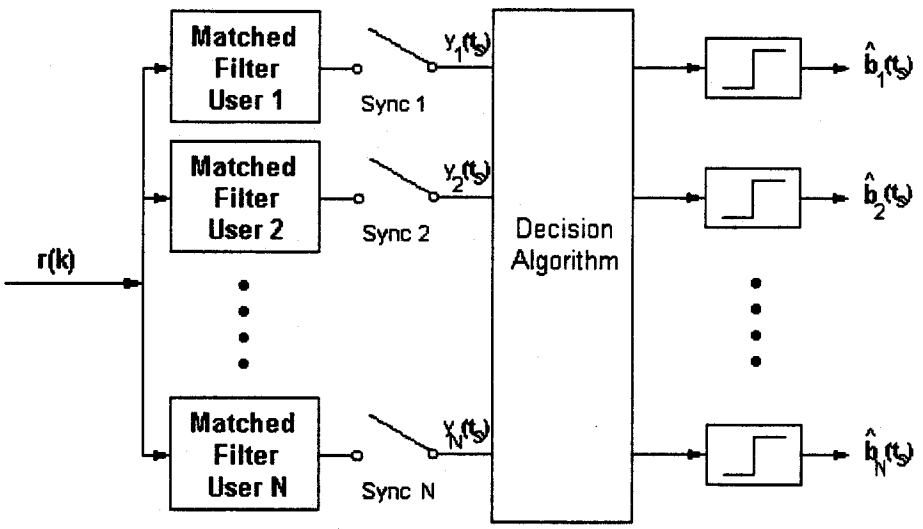

Figure 2.2: ML optimum detector.

where $\mathbf{D}_r = \text{diag}(d_1, d_2, \ldots, d_{N_r})$ is nth user's diagonal amplitude matrix. Assuming that the cross-correlation matrix $\mathbf{A}$ is invertible:

$$\begin{aligned} \mathbf{u} &= K\mathbf{A}\mathbf{D}_r\mathbf{b} + \mathbf{n} && (2.7) \\ \mathbf{A}^{-1}\mathbf{u} &= K\mathbf{A}^{-1}\mathbf{A}\mathbf{D}_r\mathbf{b} + \mathbf{A}^{-1}\mathbf{n} && (2.8) \\ &= K\mathbf{D}_r\mathbf{b} + \mathbf{A}^{-1}\mathbf{n} \end{aligned}$$

we can then recover the transmitted data $\widehat{b}_n$ by determining the sign of the nth element of $K\mathbf{A}^{-1}\mathbf{u}$ denoted as $(K\mathbf{A}^{-1}\mathbf{u})_n$,

$$\begin{aligned} \widehat{b}_n &= sgn((K\mathbf{A}^{-1}\mathbf{u})_n) && (2.9) \\ &= sgn((K\mathbf{D}_r\mathbf{b} + \mathbf{A}^{-1}\mathbf{n})_n) && (2.10) \end{aligned}$$

In the presence of noise, the decorrelating detector can completely eliminate the MAI, but at the expense of enhancing the variance of the additive white Gaussian noise (AWGN) noise. This noise enhancement is a function of the cross-correlations between the different spreading sequences and is independent of the power levels of the different signals. Therefore the decorrelating detector does not require power control.

Minimum Mean Squared Error (MMSE) Detector

The MMSE detector is a linear detector designed to compensate for the noise enhancements produced by the decorrelating detector. Thus the detector tries to minimize $E[\|\mathbf{b} - \mathbf{Wu}\|^2]$, the mean squared error between the desired data and the soft output of the conventional receiver, where $\mathbf{W}$ is shown in [8] to be:

$$\mathbf{W}_{MMSE} = [\mathbf{A} + (N_0/2)\mathbf{D}^{-2}]^{-1} \tag{2.11}$$

Applying the minimum mean square error (MMSE) detector, we obtain $\widehat{\mathbf{u}}_{MMSE} = \mathbf{W}_{MMSE}\mathbf{u}$. Comparing this result to the one obtained using the decorrelating detector, the MMSE detector implements a modified correlation inverse which takes into account both MAI and AWGN. Thus, the MMSE detector balances both MAI and AWGN to produce in general a better decision variable than the decorrelating detector. A disadvantage of this detector is that, unlike the decorrelating detector, the amplitude of the signals plays a role in determining $\mathbf{W}_{MMSE}$ increasing computational complexity compared to the decorrelator.

2.1.5 Suboptimal Non-Linear Detectors

The main underlying principle behind non-linear detectors is interference cancelation, where MAI caused by different users is estimated and subtracted from the desired user. These detectors are similar to feedback systems, where decisions on previously detected symbols are fed back in order to eliminate some of the MAI. Successive interference cancelers, multistage detectors and decision feedback detectors are among the most common types of non-linear detectors.

Successive Interference Cancelation (SIC)Detector

The general idea behind SIC is, if a decision has been made about one user's bit, its signal can be recreated and subtracted from the received signal to remove its interfering effect on other users. This will provide a way to cancel out interference provided the decision was correct and the receiver knows the signal's amplitude. Once this is done, the process is repeated for another interferer until all signals have been subtracted from the received signal. Since errors in previously detected signals play an important role in the reliability of the system, the ordering in which users are detected affects the performance. The optimal method of ordering the signals for interference cancelation is according to signal strength.

The reasoning behind this ordering is because of the advantages in MAI. When the signal is detected at the receiver the user with the strongest signal is the most likely to be detected correctly. Once removed the strongest signal gives the most cancelation benefit to other users [9] by removing the largest contributor to MAI. Figure 2.3 shows the operation of a SIC detector using conventional detectors with the first stage, sorting of the users' signals according to their powers, is not shown. The detection of the strongest user $b_1(t_s)$ is then subtracted from the received signal $\mathbf{r}(t)$, yielding a received signal $\mathbf{r}_1(t_s)$. If the estimation of the desired user is accurate, less MAI is seen in the next stages.

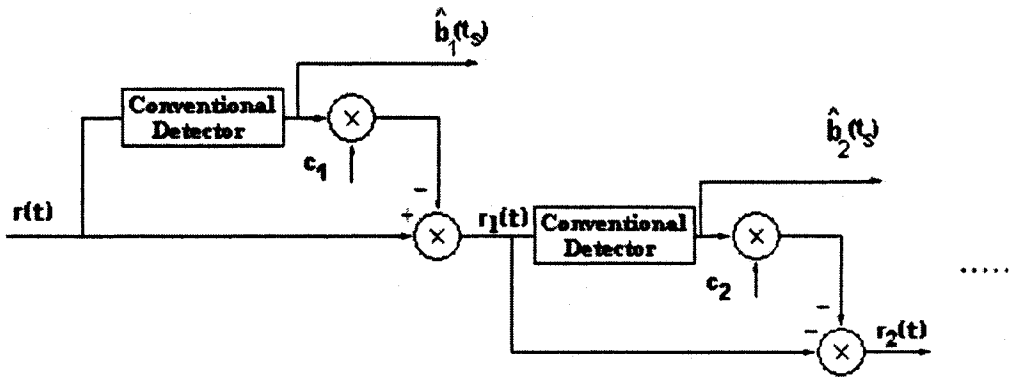

Figure 2.3: Successive Interference Cancelation Detector.

Multistage Parallel Interference Cancelation (PIC) Detector

PIC uses a parallel method to subtract out the MAI from each user. This is done by using multiple stages where the m-th stage of the detector uses decisions of the $(m-1)$th stage to cancel MAI present in the received signal. The second stage of the PIC detector is shown in Figure 2.4, where the initial stage (the conventional detector) is not shown. The initial inputs $\widehat{b}_i(t_s - T)$ are derived from the estimates of the matched filter. The amplitudes of these bits are then estimated and respread, producing a delayed estimate of the received signal. The partial summer then estimates the total MAI by summing up all the users' signals except for the desired signal and subtracts it from a delayed version of the received signal. The filtered signal is then passed though a conventional detector and a decision is made.

Some disadvantages associated with PIC include delay and power control. To cope with

delay constraints, usually the number of stages is limited to two. As for power control, if none is available weaker signals will be affected greatly by MAI subtraction. In general when comparing performance between SIC and PIC, for a system with power control PIC outperforms SIC, while for systems without power control, SIC outperforms PIC [10].

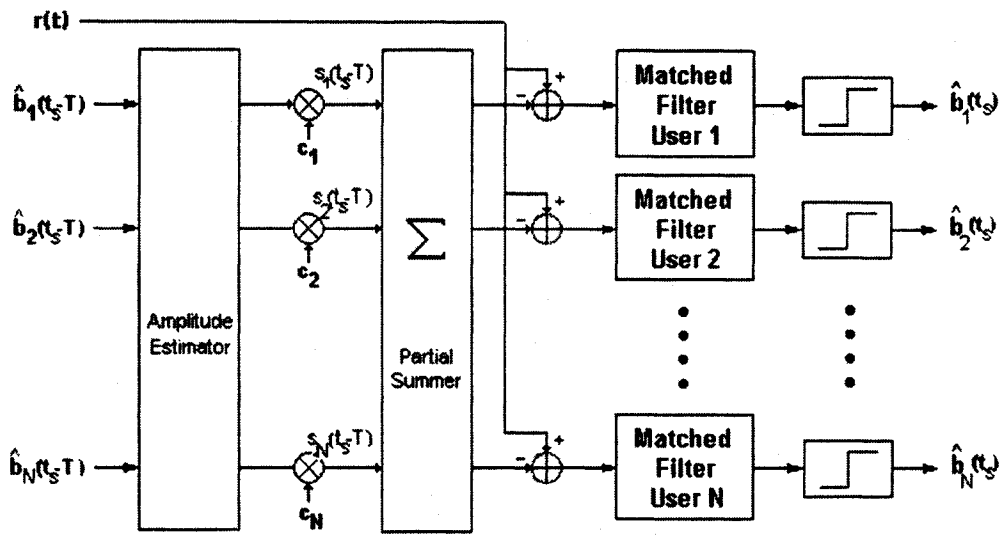

Figure 2.4: One stage of the multistage PIC detector (the initial stage is not shown).

Decision Feedback (DF) Detector

Decision feedback detectors were discussed by Duel-Hallen in [11]. They can be characterized by two operations: linear preprocessing which estimates the users' data followed by a form of SIC detection to subtract out the interference [12] and [9]. In each time interval, decisions are made in order of users' decreasing signal strength, where stronger users are detected first to allow weaker users to utilize their decisions. One of the more popular DF detectors, shown in Figure 2.5, is the zero-forcing decision-feedback detector. Following the sorter (where users are ranked according to signal power), a noise whitening filter $\mathbf{G}_w$ (obtained using Cholesky factorization) is applied [13]. Decisions are made using the SIC operation and then subtracted out at the next signal period in order of decreasing signal power.

In a white noise model the data bits become partially correlated, where the output from the first user contains no MAI and the output from the second user contains MAI from the

first while being completely decorrelated from all other users, etc. The ZF detector then uses SIC detector to remove the first user's detected bit to cancel out the MAI it produces.

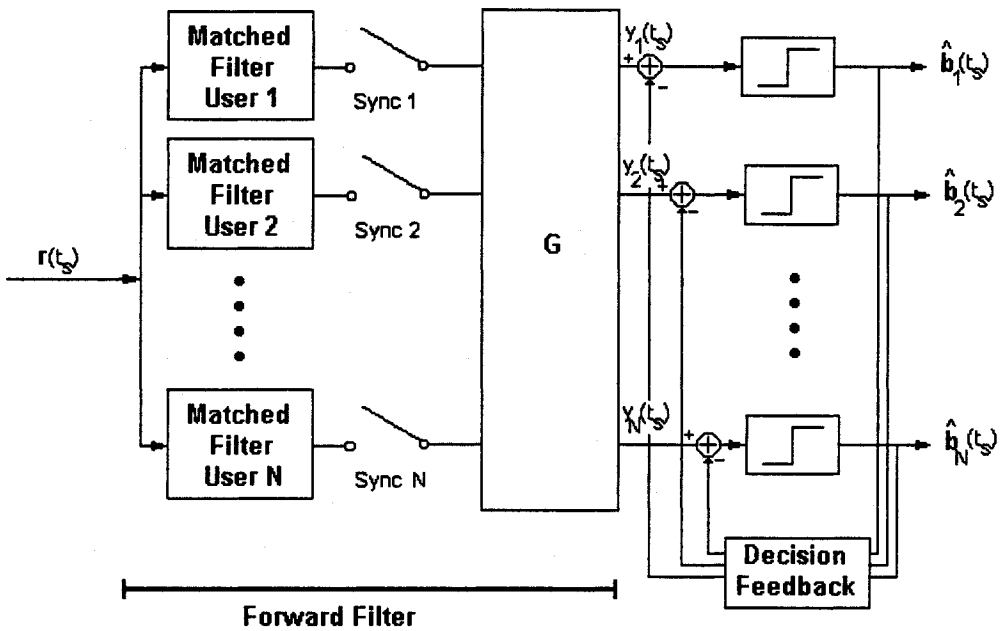

Figure 2.5: Decision feedback detector.

2.1.6 Partial Decision Variable Technique

In [3] it proposed employing linear adaptive filters to produce multiple decision variables with improved signal to interference ratio. To detect each PDV, the conventional technique is sub-divided into the following sub-signaling intervals:

$$\begin{aligned} u_n &= \int_0^{T_b} 2r(t)c_n(t)cos2\pi f_c t dt \\ &= \sum_{x=1}^{X} \int_{\frac{(x-1)T_b}{X}}^{\frac{xT_b}{X}} 2r(t)c_n(t)cos2\pi f_c t dt \\ &= \sum_{x=1}^{X} \mathbf{U}_{n,x} \end{aligned} \tag{2.12}$$

where T_b is the signal duration and f_c is the carrier frequency. Then instead of summing X PDVs, we can compute a weighted sum of each decision variable to a single decision variable which maximizes SINR:

$$y_n = \sum_{x=1}^{X} w_{n,x} \mathbf{U}_{n,x} \tag{2.13}$$

where $w_{n,x}$ is the xth weight found using linear adaptive filters for the nth user's decision variable. These filters employ the LMS algorithm along with decision feedback for each weight. These outputs can then be used to make a hard decision or become soft inputs to other sub-optimal detectors. Overall, results show that using PDVs provide some improvements to the BER performance of the system. Therefore by only slightly increasing the complexity of the system, additional power gain can be obtained by employing PDVs.

2.2 CDMA Systems Employing Multiple Antennas

It has been recognized that the use of multiple transmit and receive antennas increases diversity over traditional single input single output (SISO) systems. By employing multiple transmit and receive antennas in a CDMA environment, we expect significant BER performance gain. In this section we look at recent research in the area of multiple antenna CDMA systems.

2.2.1 SIMO CDMA System

To improve performance researchers looked at different diversity techniques. By employing multiple antennas at the receiver, diversity can be obtained having a single transmitter send its signal through a multipath environment to create differently faded versions of the signal at each receiver antenna [14]. Previous work has addressed the integration of multiuser receivers with antenna arrays in AWGN channels [15, 16]. Miller [15] presented the optimal receiver structure, where each antenna performs spatial processing, followed by a bank of matched filters using adaptive distributed multiuser algorithms.

One year later the combination of an adaptive antenna array and interference canceler was proposed by Kohno [16]. Similar ideas have been proposed by Cho [17] and Horng [18], showing significant BER performance improvements in a Rayleigh fading channel. Cho proposed a digital receiver for DS-CDMA detection in [17] by exploiting the space diversity and adaptive interference cancelation to mitigate the effects of channel fading and MAI.

The receiver consists of multiple diversity antennas and adaptive interference cancelers in conjunction with simple selection combining. Simulation results showed that for a moderately loaded system (10-12 users) and 4 diversity antennas, a significant BER performance improvement can be achieved. In [18], Horng presented a similar idea to [17] which employs diversity combining rather than selection diversity, providing simple detection techniques.

Linear detectors have also received attention, for example in [19] Yuan extended adaptive distributed multiuser algorithms [15] to include a decorrelating detector and a blind adaptive diversity-combining scheme at the receiver. The advantages of using this implementation include eliminating the multipath interference, introducing near-far resistance, providing error rate performance improvement and increasing system capacity. Using theoretical analysis and simulations, Yuan showed that by using the blind adaptive combining scheme, weights efficiently converge to the optimum weighting, while obtaining an error performance similar to that of the maximum ratio scheme with less complexity.

2.2.2 MIMO CDMA System

With the introduction of multiple input multiple output (MIMO) systems that employ multiple transmit and receive antennas, systems can exploit spatial diversity by transmitting/receiving through multiple antennas. This additional diversity can be provided only if the antennas are spaced far enough apart that signals from each antenna undergo independent fading. This distance however can be misleading, as shown in [20] with the use of measured data these distances may be unreasonably large. However, in the ideal case MIMO channel models are assumed to be uncorrelated. The main techniques already proposed to exploit MIMO systems are: space-time block codes (STBC), introducing redundancy across multiple antennas [21]; and spatial multiplexing (SM), which transmits multiple data symbols simultaneously from different antenna elements [22].

By implementing STBC in DS-CDMA we can achieve high performance through diversity and coding gains through spatial and temporal redundancy. In [23] and [24], novel decoding algorithm were presented applying STBC to a DS-CDMA system. Zhang [23] took into account multipath components, in which the proposed algorithm constructs a symbol by symbol detector to realize ML detection. Through numerical simulations, they were able to achieve good performance with relatively low SNR and large number of users. Kou [24] showed similar performances implementing STBC with different system configurations.

Another method for improving performance is to use MUD with STBC-CDMA system, which are referred to as space-time multiuser detectors (ST-MUD) [25–28]. In [25] a space-

time SIC scheme in Rayleigh fading channels was presented. Utilizing Alamouti's code [29] a low complexity system was designed. Wei [26] used a similar approach implementing STBC-CDMA with an SIC algorithm with a modified sorting algorithm. Results showed by using the novel technique, MAI is greatly reduced and hence the system has better performance. Linear algorithms can also be implemented. In [28], the decorrelating detection algorithm was chosen as the MUD scheme. Even though performance was good, computational complex was high due to existence of the matrix inverse operation.

In regards to studies on spatial multiplexing CDMA systems, the literature is very limited. One study in [30] determined capacity of MIMO-CDMA system with SM and a modified V-BLAST algorithm. Results showed that in a multi-user multi-antenna system the capacity grows linearly with the number of antennas, similar to the single user system. Furthering that study, Wan [27] examined the effectiveness of SM with a low complexity linear receiver, showing both numerical and theoretical results to coincide and outperform the conventional SISO-CDMA system.

Chapter 3

System Model

3.1 Proposed PDV System

This thesis investigates the performance of PDVs in a synchronous DS-CDMA system in the presence of slow varying frequency-nonselective Rayleigh fading (discussed later in this chapter). With the PDV technique the detector produces multiple decision variables for every symbol for each user by considering the received signal over non-overlapping intervals of duration that is a fraction of the symbol interval [3], creating X PDVs. Figure 3.1 shows a block diagram of the proposed technique. At the receiver, instead of taking the limits of summation over the entire information period, the receiver divides the information interval into multiple smaller detection subintervals and PDVs are generated for each. The PDVs are then weighted, using adaptive algorithms discussed in Chapter 3 to find the weight vector $\mathbf{w} = [w_1, w_2, ..., w_X]$, according to their respective SINRs and combined, improving the overall SINR and hence BER. Equation (1.3) can be modified to account for PDVs as:

$$u_{n,x} = \sum_{j=1}^{N} h_j b_j \sum_{k=(x-1)K/X}^{xK/X} c_n(k) c_j(k) + \eta_x \tag{3.1}$$

for the subinterval x and η_x is the corresponding matched filter's response to the white Gaussian noise. The above expression can be rewritten in matrix form as follows:

$$\begin{bmatrix} u_{1,x} \\ u_{2,x} \\ \vdots \\ u_{N,x} \end{bmatrix} = K \begin{bmatrix} 1 & \rho_{12,x} & \dots & \rho_{1N,x} \\ \rho_{12,x} & 1 & \dots & \rho_{2N,x} \\ \vdots & \vdots & \ddots & \vdots \\ \rho_{1N,x} & \rho_{2N,x} & \dots & 1 \end{bmatrix} \cdot \begin{bmatrix} h_1 & 0 & \dots & 0 \\ 0 & h_2 & \dots & 0 \\ \vdots & \vdots & \ddots & \vdots \\ 0 & 0 & \dots & h_N \end{bmatrix} \cdot \begin{bmatrix} b_1 \\ b_2 \\ \vdots \\ b_N \end{bmatrix} + \mathbf{n}_x \tag{3.2}$$

where $\rho_{nj,x}$ is the cross-correlation between code sequences n and j in the xth subinterval. This can be written concisely as:

$$\mathbf{u}_x = \frac{K}{X}\mathbf{A}_x\mathbf{D}\mathbf{b} + \mathbf{n}_x \tag{3.3}$$

where $\mathbf{A}_x$ is such that $[A_x]_{n,j} = \rho_{nj,x}$ and $\mathbf{D}$ is the diagonal complex channel gain matrix.

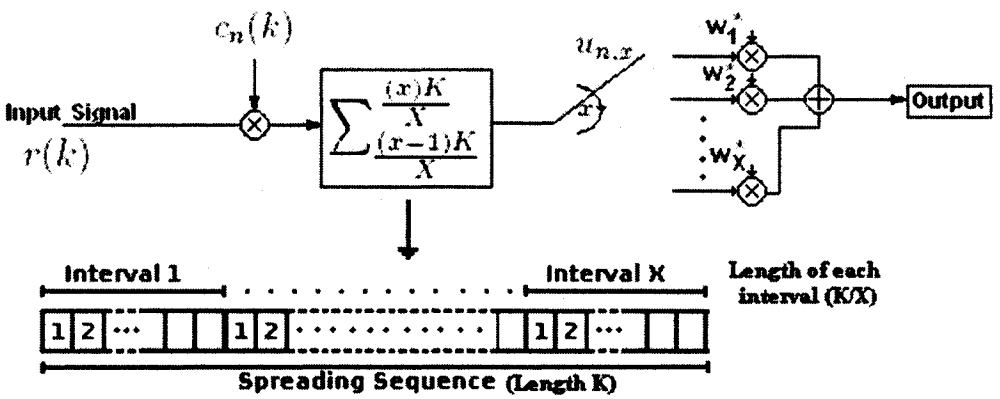

Figure 3.1: Baseband equivalent block diagram of the PDV technique using X decision variables at the detector of one user.

3.2 Partial Decision Variable (PDV) Technique using Multiple Receive Antennas

In this thesis, we have assumed that binary phase shift keying (BPSK) modulation is used for transmission. At the detector, the received signal would be that of (3.1). We consider a DS-CDMA system which consists of N users and N_r receive antennas. If we use the PDV technique, over the xth signaling subinterval, each user is detected such that in matrix form it is similar to (3.3) but instead of a decision variable being made from only one antenna, N_r receive antennas are used for user n:

$$\begin{bmatrix} \mathbf{u}_{x,1} \\ \mathbf{u}_{x,2} \\ \vdots \\ \mathbf{u}_{x,N_r} \end{bmatrix} = \frac{K}{X} \begin{bmatrix} \mathbf{A}_{x,1}\mathbf{D}_1 \\ \mathbf{A}_{x,2}\mathbf{D}_2 \\ \vdots \\ \mathbf{A}_{x,N_r}\mathbf{D}_{N_r} \end{bmatrix} \cdot \begin{bmatrix} b_1 \\ b_2 \\ \vdots \\ b_n \end{bmatrix} + \mathbf{n} \tag{3.4}$$

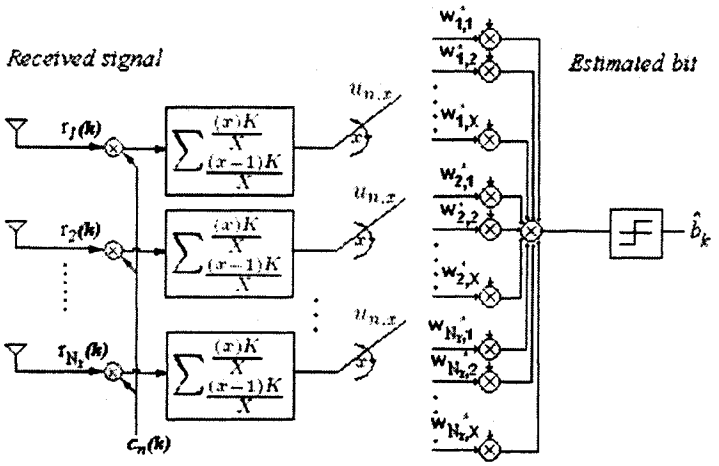

Figure 3.2: PDV technique using multiple antennas and adaptive weights

where $\mathbf{A}_{x,n_r}$ and $\mathbf{D}_{n_r}$ are the code correlations and diagonal channel matrix defined in (3.2), where the subscripts n_r and x denote the matrix for a certain diversity path and signaling subinterval respectively. Now each decision vector $\mathbf{u}_{x,n_r}$ represents every user's decision variables on a selected diversity path. Therefore instead of having a decision variable as a vector of length N, the decision variable has become a vector of length $N \cdot N_r$. The advantage of using additional antennas in conjunction with PDVs is the introduction spatial diversity. Using spatial diversity, if one signal experiences more fading from one antenna then another, this will be compensated by the detector where the LMS algorithm will weight each PDV to minimize the minimum mean square error (MMSE).

Figure 3.2 illustrates the complete PDV system using adaptive weights. From the figure, each antennas utilizes the PDV technique independently creating X decision variables. These decision variables in conjunction with PDVs from other receive antennas are weighted to produce a single decision variable.

3.3 Channel Models

In [3] results show that the use of PDV provides improvement to the overall BER performance of the system in a geo-satellite system, representing the best case scenario for a signal at the receiver. This thesis will extend work done in [3] for a quasi-static Rayleigh fading channel, a Rayleigh flat fading channel, and real channels using measured channel data.

3.3.1 Static Frequency Nonselective Fading Model

Figure 3.3 depicts a general mobile scenario. For the ideal case, when we consider the channel to be constant over the duration of transmission, we only need to consider multipath propagation. The received signal $r(t)$ can arrive at the receiver from multiple directions with different propagation delays and amplitudes such that:

$$r(t) = \sum_{i=1}^{M} r_i cos(\omega t + \varphi_i) \tag{3.5}$$

where M is the number of received signals and φ_i is the angle of arrival. We can then simplify the above equation as:

$$r_i cos(\omega t + \varphi_i) = r_x cos(\omega t) - r_y sin(\omega t) \tag{3.6}$$

and $r_x = \sum_{i=1}^{N} r_i cos(\varphi_i)$ and $r_y = \sum_{i=1}^{N} r_i sin(\varphi_i)$ are the in-phase and quadrature components. Then the amplitude of the received signal $r = \sqrt{r_x^2 + r_y^2}$ is Rayleigh distributed assuming that r_x and r_y are i.i.d. amplitude components and the $\varphi_i \in [0, 2\pi)$ are i.i.d. phase components.

3.3.2 Small-Scale (Multipath) Fading Model

Small-scale fading is used to describe the fluctuation of a signal over a short period of time, such that path-loss effects are ignored. Small-scale fading or multipath fading is a phenomenon that causes multiple versions of the transmitted signal to arrive at the receiver, each having their own phase, angle of arrival and amplitude. These signals, when combined at the receive antenna, will produce a resultant signal which has varying amplitude and phase.

In a typical microcell propagation environment, small-scale fading occurs because the mobile transmitter and base-station receiver are located below the surrounding structures such that no line of sight is available. Even though the movement and location of the mobile receiver and/or transmitter cause degradation in system performance, when considering a static transmitter and receiver, the received signal fade due to movement in surrounding objects. The following lists factors that can influence small-scale fading:

Multipath propagation - While situated in a urban environment buildings, cars and other objects can reflect and/or scatter the transmitted signal, varying its amplitude, time and phase. These effects result in multiple copies of the transmitted signal arriving at different times and spatial orientation, introducing small-scale fading.

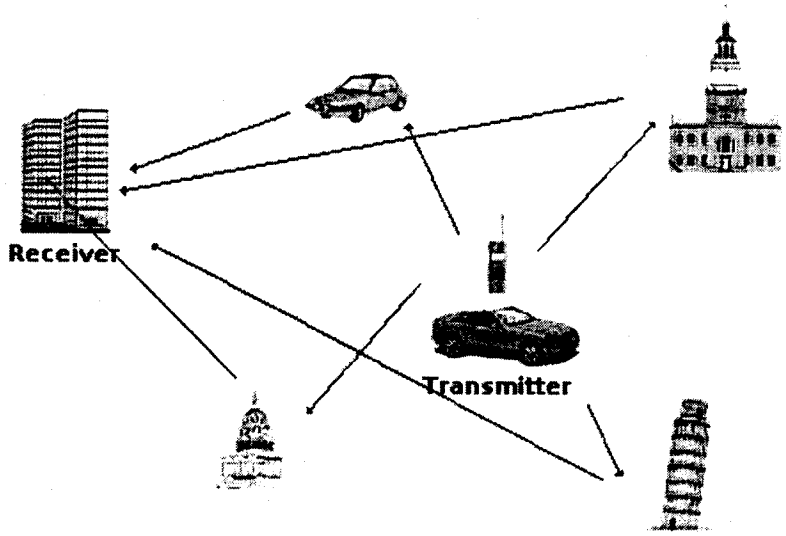

Figure 3.3: Typical microcell propagation environment.

Speed of mobile - When a mobile is in motion, a resulting random frequency shift occurs on the modulated signal due to the Doppler effect (which will be described later in this chapter). This shift will either be positive or negative depending on the mobile's direction of travel compared to the base-station.

Speed of surrounding objects - While the speed of a mobile can effect the received signal, so can the surrounding objects. If these objects move at a much faster rate than the mobile, they can induce a Doppler shift on multipath components.

Transmission bandwidth of signal - Each multipath channel has a maximum frequency range for which signal amplitudes can remain highly correlated. In other words, if the bandwidth of the transmitted signal is greater then the maximum bandwidth (BW) or coherence bandwidth the amplitude of the received signal will be distorted.

The above factors can drastically alter the characteristics of a multipath channel. In the section below, different models are presented to try and characterize the effects of multipath fading. Equation (3.5) represents a very simplified model of a mobile channel which does not

consider movement of the mobile receiver. When dealing with receivers in motion, the signal in relation to the transmitted signal will undergo different types of small-scale fading [1].

Multipath Time Delay Spread

Multiple reflections of the transmitted signal may arrive at the receiver over a certain time interval which at times can result in inter symbol interference (ISI). This time dispersion of the channel is called multipath time delay spread. Some common parameters often calculated when referring to multipath delay spread are the root mean square (RMS) delay spread, mean excess delay and excess delay spread.

When dealing with delay spread, a parameter commonly used to characterize fading is coherence bandwidth B_c. Coherence bandwidth, derived from the RMS delay spread, is a statistical measure of the range of frequencies over which the channel is considered flat. In other words, the coherence bandwidth is the range in frequency in which all spectral components have approximately the same gain and phase. For example, if two signals being transmitted have a frequency separation greater than B_c, the effects on each signal due to the channel will be quite different.

Doppler Effect

When dealing with propagating waves, movement in the receiver or transmitter will distort the perceived signal's frequency. This phenomenon known as the Doppler effect is present in any mobile system. Consider a mobile receiver moving at a constant velocity v. Let us assume that the source is far enough away so that the angle of arrival can be considered constant over a short period of time. We can calculate the excess distance the signal needs to travel $\Delta l = v(t)\Delta t cos\theta$ (where θ is the angle between the direction of travel and the direction of the transmitter to the receiver), which is relative to the distance the mobile has moved in time Δt. The resulting phase difference is then:

$$\Delta\phi = \frac{2\pi\Delta l}{\lambda} = \frac{2\pi\nu\Delta t}{\lambda} cos\theta \tag{3.7}$$

where λ is the wavelength in meters. Hence the Doppler shift f_d can be found to be:

$$f_d = \frac{1}{2\pi} \cdot \frac{\Delta\phi}{\Delta t} = \frac{\nu}{\lambda} \cdot cos\theta \tag{3.8}$$

Figure 3.4 illustrates the effect of motion on different frequency shifts. As the transmitter moves towards to the receiver the frequency of the signal increases and vice versa.

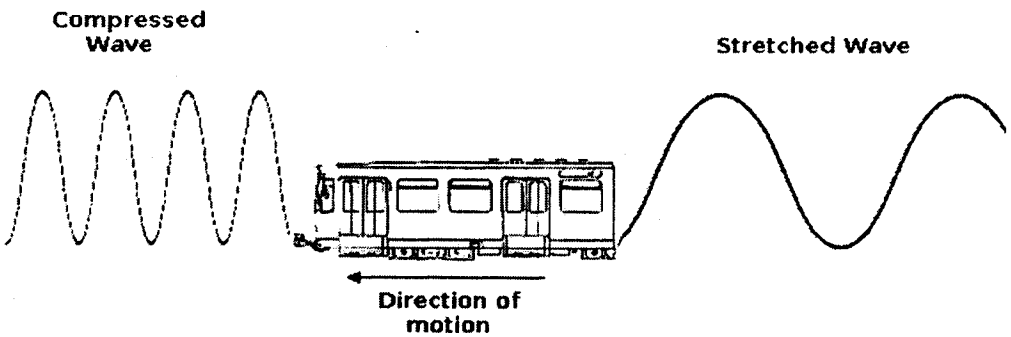

Figure 3.4: Illustration of Doppler effect.

In mobile communications Doppler spread and coherence time are two parameters which describe the time varying nature caused by the Doppler effect. Doppler spread B_d, defined as the range of frequencies over which the Doppler spectrum is non-zero, is caused by the rate of change in a mobile channel. To describe this phenomenon, when a pure sinusoidal of frequency f_c is transmitted through a multipath fading channel, the received signal will have components distributed in the range of $f_c - f_d$ and $f_c + f_d$ similar to the one shown in Figure 3.6 where f_d is the Doppler shift. As shown earlier, f_d is a function of the velocity and the angle between the direction of motion of the mobile and the direction of arrival at the receiver.

Coherence time T_c is a common parameter used when characterizing a fading channel. This parameter, which is approximately the inverse of the maximum Doppler spread, measures the time duration over which the channel impulse response may be considered constant. This means that if the received signal has a reciprocal bandwidth greater than the coherence time of the channel, the channel will change during transmission.

Types of Small-Scale Fading

In the previous section, we looked at different types of fading experienced in a mobile channel. Depending on the characteristics of received signal (such as bandwidth and symbol period) and the characteristics of the channel (such as coherence bandwidth and coherence time), different signals will experience different types of fading. Figure 3.5 summarizes the different types of small-scale fading and a general description of each is given below. For fading based on multipath time delay and Doppler spread, they each have two types:

Frequency-Nonselective (Flat) Fading, where the coherence bandwidth of the channel

B_c is greater than the bandwidth of the signal W, meaning the delay spread T_c is less than the symbol period T.

Frequency-Selective Fading, where the coherence bandwidth of the channel is less than the signal, meaning the delay spread is greater than the symbol period.

Fast Fading, where Doppler spread is high and the coherence time is less than the symbol period, i.e., the channel variations are faster than the baseband signal variations.

Slow Fading, where Doppler spread is low and the coherence time is much greater than the symbol period, having channel variations slower than the baseband signal variations.

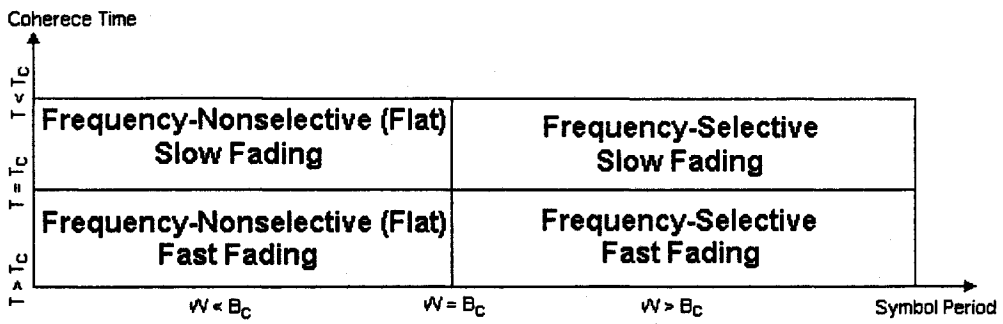

Figure 3.5: Different types of small-scale fading.

In this thesis, using the method described below we simulated a slowly fading frequency nonselective Rayleigh fading channel.

3.3.3 Simulating Flat Fading Channel Models (Clarke's Model)

Over the years several statistical models have been designed to try and describe the nature of the mobile channel. One of the first, proposed by Ossana [31] predicted flat fading signals, which agreed with measurements where line of sight is available. One of the more widely used models today is Clarke's model [32], based on scattering. In [32] it was shown that given a model that assumes a fixed transmitter with a vertically polarized mobile receive antenna detecting M scatterers with arbitrary carrier phases and arbitrary angles of arrival, by increasing M the random received signal envelope r has a Rayleigh distribution, in the absence of line of sight.

Another useful representation of this model was developed by Gans [33], using a statistical

approach he modeled the fading spectrum of Clarke's model as:

$$S(f) = \frac{A[p(\alpha)G(\alpha) + p(-\alpha)G(-\alpha)]}{f_d\sqrt{1-(\frac{f-f_c}{f_d})^2}} \tag{3.9}$$

where f_c is the carrier frequency, f_d is the maximum Doppler frequency, $G(\alpha)$ is the azimuthal gain pattern of the mobile antenna as a function of the angle of arrival, and $p(\alpha)$ denotes the fraction of the total incoming power as a function of angle of arrival. Figure 3.6 shows the power spectrum of the mobile receiver defined in equation (3.10), for the case of a vertical $\lambda/4$ omnidirectional antenna ($G(\alpha) = 1.5$), and a uniform distribution $p(\alpha) = 1/2\pi$ over 0 to 2π, given by

$$S_E(f) = \frac{1.5}{\pi f_d\sqrt{1-(\frac{f-f_c}{f_d})^2}} \tag{3.10}$$

where we have plotted the spectrum vs. offset from f_c. In our simulations we considered the signal at baseband where $f_c = 0$.

Simulation of multipath fading channels is needed to evaluate the performance of our proposed system. A method based upon Smith's model [34], uses in-phase and quadrature components paths to simulate a signal representing equation (3.10). The main principle behind Smith's method is shown in Figure 3.7. For our simulation, we use the spectral filter defined in (3.10) to shape complex white Gaussian low pass noise sources in the frequency domain to produce coloured Gaussian noise modeling the fading spectrum. Then by applying the inverse fast Fourier transform (IFFT), an accurate model of a fading time domain channel with Doppler spread is produced.

Figures 3.8 and 3.10 show typical multipath fading envelope for Doppler frequencies of 5Hz and 50Hz with a sampling rate of 1000 samples/sec. From the figures the results relate directly to theoretical results, where as we increase the maximum Doppler frequency the frequency which the signal fades also increases. Also when looking at the histogram of the amplitudes the distribution is Rayleigh. In this thesis we simulated a Rayleigh flat fading channel, using a Doppler frequency of 5Hz to represent the speed of slow moving mobile users and 1000 samples/sec as the receiver's sampling rate.

3.3.4 Real Channel Data

Channel data used in this thesis was obtained by the Radio Communications Technologies group at CRC. Using a MIMO configuration with N_t transmit and N_r receiver antennas,

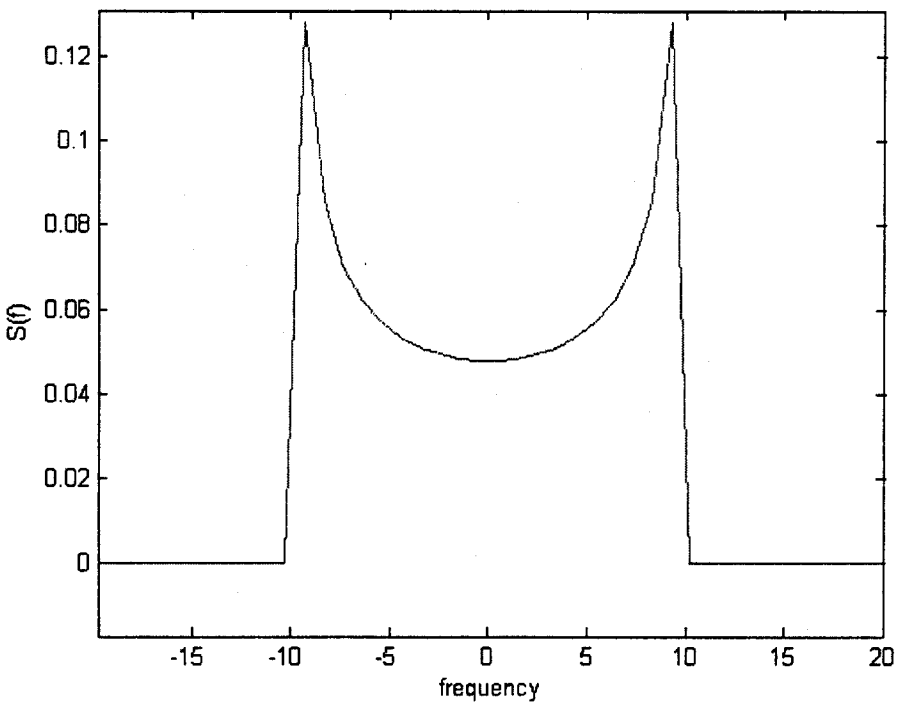

Figure 3.6: Illustration of fading spectrum for a Doppler spread of 10Hz.

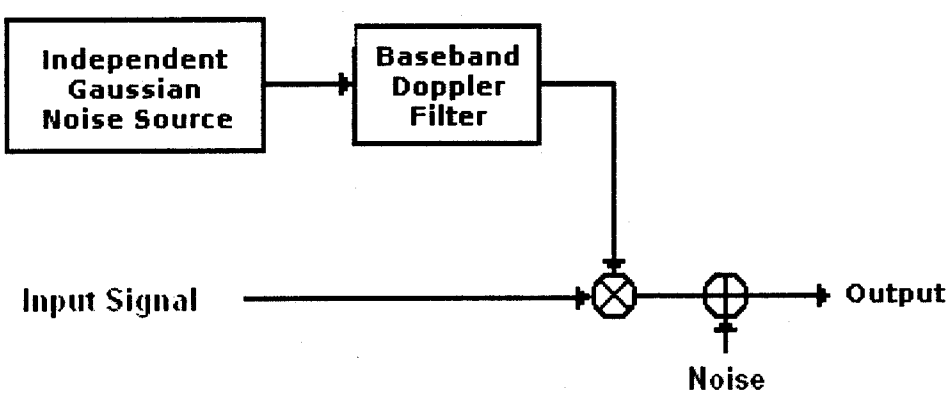

Figure 3.7: Baseband Doppler filter model.

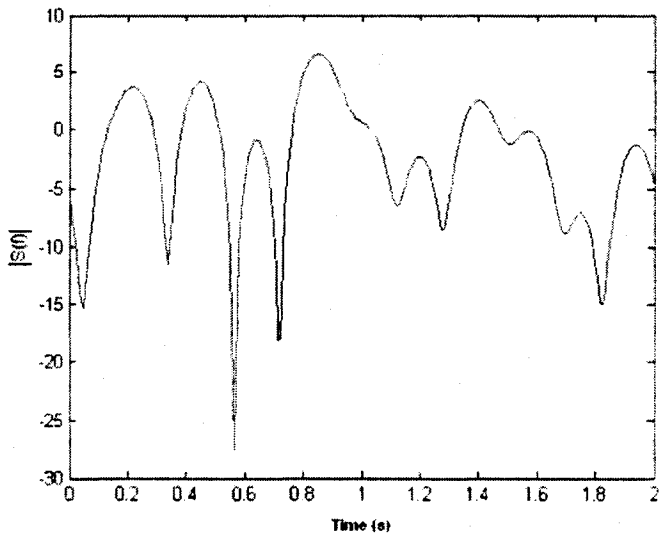

Figure 3.8: Magnitude of multipath fading channel at $f_d = 5$Hz

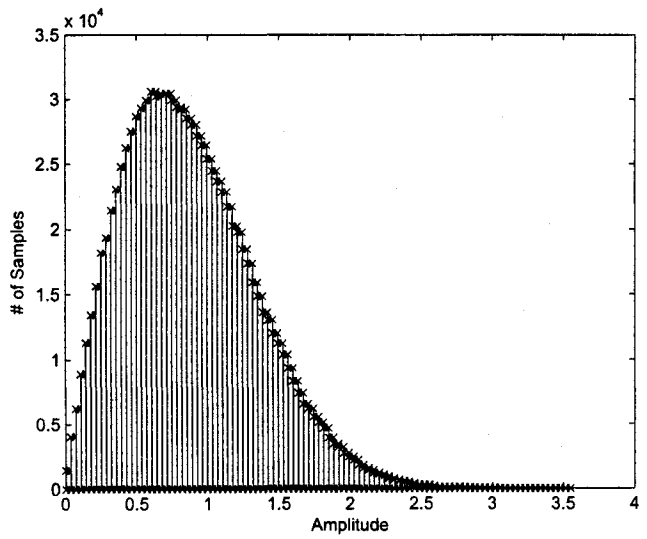

Figure 3.9: Histogram of multipath fading channel at $f_d = 5$Hz.

$N_t = 4, N_r = 4$, measurements were taken throughout downtown Ottawa, Canada. In all measurements the transmitter was located at a fixed location inside a building, while the receiver traveled on a van at approximately 30km/hr through the downtown core. Using om-

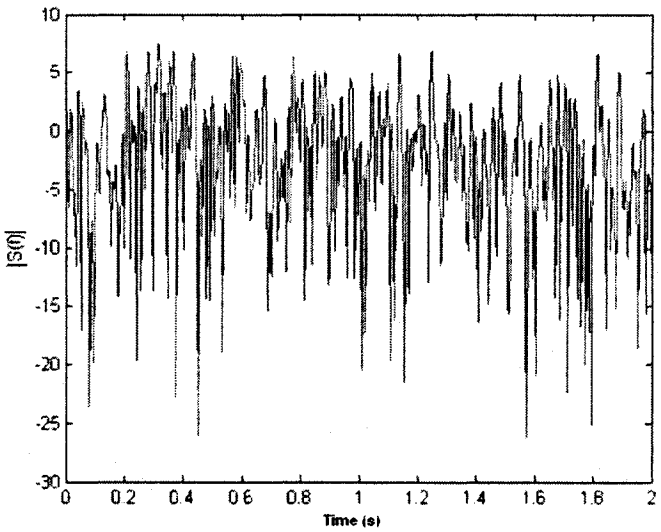

Figure 3.10: Magnitude of multipath fading channel at $f_d = 50$Hz.

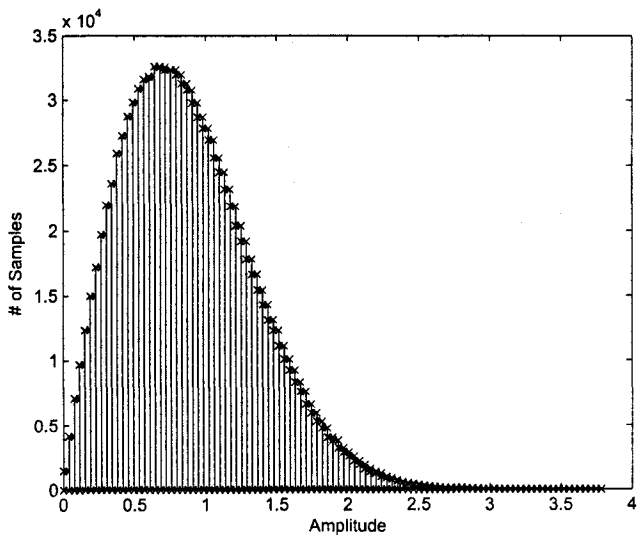

Figure 3.11: Histogram of multipath fading channel at $f_d = 50$Hz.

nidirectional, vertically-polarized monopole antennas at the transmitter, a repeating pseudo-noise sequence was transmitted and received. With custom built hardware/software to provide amplification and down-conversions, sampling of the channel's in-phase and quadrature

components were recorded at a sampling rate of 50Msamples/sec. A more detailed description of the channel measurement equipment and the corresponding channel data is in [20] and [35].

3.4 Diversity

When transmitting a signal the probability of encountering a deep fade is relatively high. However if several replicas of the desired signal propagate over independently fading channels, then the probability that all replicas encounter deep fades simultaneously is very low [14]. Therefore, by having more than one path to select from, both the instantaneous SNR and average SNR can drastically improve.

There are many different diversity techniques. One method is employing frequency diversity, where different carriers are used to transmit the same information. The disadvantage of this technique is its inefficient use of bandwidth. Time diversity is another method where the same information is transmitted over different time slots. It is shown in [36] that using repetition coding is inefficient in its use of bandwidth when compared with coding. A third technique is to employ multiple antennas arrays (space diversity) where the antennas are significantly separated so that the correlation of the fading process is low. Other diversity techniques have been proposed in the literature (e.g. [37–39]) such as: polarization diversity and angle of arrival diversity but have not been as widely used as those described above. In this thesis our main focus will be on space diversity.

3.4.1 Selection Diversity Combining

Selection diversity is the simplest of the space diversity techniques. Using an array of antennas, the receiver samples each antenna signal [40]. A comparator then compares the instantaneous SNR or SINR of each antenna and selects the signal with the highest SNR. Using this technique we are able to obtain the probability that at least one of the instantaneous SNR γ_i is greater then γ as:

$$Pr[\gamma_i > \gamma] = 1 - (1 - e^{-\gamma/\gamma_o})^{N_r} \tag{3.11}$$

where γ_o is the average SNR. In most cases the performance of this technique is quite poor, especially when the average signal strength on all antennas is equal. The advantage of this technique is its low complexity.

3.4.2 Maximum Ratio Diversity Combining

Proposed in [14], maximum ratio diversity provides the optimum diversity combining law for coherent detection. Using individual weights for each antenna in the array, N_r branches are weighted according to their received SNR. Unlike selection diversity, maximum ratio combining (MRC) uses linear coherent combining of each individual signal with weights so that the output SNR is maximized, yielding

$$Pr[\gamma_i > \gamma] = 1 - (1 - e^{-\gamma/\gamma_o}) \sum_{k=1}^{N_r} \frac{(\gamma/\gamma_o)^{k-1}}{(k-1)!}. \tag{3.12}$$

This technique gives the best statistical reduction of fading known to any linear detectors, but it is also the most complex.

3.4.3 Equal Gain Diversity Combining

In many cases when MRC is too complex for implementation, equal gain combining (EGC) [14] provides a method to allow for similar performance with less complexity. In EGC each individual antenna is given equal weighting and combined coherently, producing a single decision variable.

3.4.4 Comparisons

In selecting the appropriate combining techniques, many factors have to be considered [14, 41]. Using MRC provides the overall best performance but at the cost of the highest complexity. Implementing selection diversity is the simplest form of combining but performance of this system is poor when signals arriving are at equal strengths. Finally by using EGC the opposite of selection diversity occurs. When all signals arriving at the receiver are of the same strength equal gain combining is equivalent to MRC, but as soon as there is any fluctuation in one path relative to another, EGC is inferior to MRC. In this thesis we will be using MRC to find the optimum weights.

3.5 Summary

In this chapter, we gave a detailed description of our system model, previewing the PDV technique and how it was extended in this thesis. Furthermore, different types of multipath

fading were investigated and modeled to help us better simulate the mobile environment. In Chapter 4, we will use the models described in this chapter to simulate our results.

Chapter 4

Adaptive Algorithms

4.1 Introduction to Adaptive Algorithms

In this chapter we focus our discussion on adaptive algorithms and how they apply to the PDV technique. For a given adaptive algorithm a training signal $d(t_s)$, known to both the transmitter and receiver, is transmitted across an unknown channel and detected at the receiver. Using a training sequence of length T_l adaptive algorithms compute the optimal weighting w_{opt}, after which information bits can be detected using the optimum weights found during the training sequence to process the received signal.

4.2 Optimum Weighting

For the PDV technique described in Section 2.1, a weighting vector is chosen to optimize the decision variable according to given criteria. This can be done through the use of adaptive algorithms which train the combiner to maximize the SINR. Adaptive algorithms provide an advantage when used with antenna arrays, using multiple copies of the received signal to produce a single optimized decision variable. In general for a CDMA system with multiple receive antennas, we denote the received signal $\mathbf{u}$ as:

$$\begin{bmatrix} r_1(k) \\ r_2(k) \\ \vdots \\ r_{N_r}(k) \end{bmatrix} = \begin{bmatrix} h_1(k) \\ h_2(k) \\ \vdots \\ h_{N_r}(k) \end{bmatrix} s(k) + \mathbf{n}(k) \tag{4.1}$$

$$\mathbf{u}_n(t_s) = \begin{bmatrix} u_{1,1}(\frac{t_s}{X}) \\ u_{1,2}(\frac{2t_s}{X}) \\ \vdots \\ u_{1,X}(t_s) \\ \vdots \\ u_{2,X}(t_s) \\ \vdots \\ u_{N_r,1}(\frac{t_s}{X}) \\ u_{N_r,2}(\frac{2t_s}{X}) \\ \vdots \\ u_{Nr,X}(t_s) \end{bmatrix} = \begin{bmatrix} \sum_{k=0}^{\frac{K}{X}-1} r_{1,1}(k)c_i(k) \\ \sum_{k=\frac{K}{X}}^{\frac{2K}{X}-1} r_{1,2}(k)c_i(k) \\ \vdots \\ \sum_{k=\frac{(X-1)K}{X}}^{K-1} r_{1,X}(k)c_i(k) \\ \vdots \\ \sum_{k=\frac{(X-1)K}{X}}^{K-1} r_{2,X}(k)c_i(k) \\ \vdots \\ \sum_{k=0}^{\frac{K}{X}-1} r_{N_r,1}(k)c_i(k) \\ \sum_{k=\frac{K}{X}}^{\frac{2K}{X}-1} r_{N_r,2}(k)c_i(k) \\ \vdots \\ \sum_{k=\frac{(X-1)K}{X}}^{K-1} r_{N_r,X}(k)c_i(k) \end{bmatrix} \tag{4.2}$$

where $\mathbf{u}(t_s)$ is the decision variable of N_r receive antennas with channel gains $\mathbf{h}(t_s)$ and n is the user of interest. Then the output of the detector can be represented as:

$$y_n(t_s) = \mathbf{w}_n^H(t_s)\mathbf{u}_n(t_s) \tag{4.3}$$

where $\mathbf{w}$ is the complex weighting vector used to optimize the combination of the array elements:

$$\mathbf{w}_n^H = [\ w_{1,1}^* \quad w_{1,2}^* \quad \cdots \quad w_{1,X}^* \quad \cdots \quad w_{2,X}^* \quad \cdots \quad w_{N_r,1}^* \quad w_{N_r,2}^* \quad \cdots \quad w_{Nr,X}^*\ ] \tag{4.4}$$

where $(.)^H$ is the Hermitian operation that takes the conjugate transpose of a matrix. The weight vector $\mathbf{w}$ in our simulations and modeling is chosen such that it minimizes the mean square error (MSE) between the training sequence and the corresponding decision variables, i.e.,

$$E[|e(t_s)|^2] = E[|d(t_s) - y(t_s)|^2]. \tag{4.5}$$

The optimum weighting was introduced by Wiener and Hopf [42] by a set of equations called the Wiener-Hopf equations, which is given for a desired user n as:

$$\mathbf{w}_{opt} = \mathbf{R}^{-1}\mathbf{p} \tag{4.6}$$

where $\mathbf{R} = E\{\mathbf{u}(t_s)\mathbf{u}^H(t_s)\}$ is the autocorrelation of the received signal vector and $\mathbf{p} = E\{\mathbf{u}(t_s)d^*(t_s)\}$ is the cross-correlation vector between the desired response and the received signal. Therefore, calculating the optimum weight vector $\mathbf{w}$ by using the Winer-Hopf equations requires knowledge of the statistics of the input vector $\mathbf{u}$ and the desired signal d which are not feasible, this is why sub-optimal weighting is needed.

4.3 Sub-Optimal Weighting

4.3.1 Sub-Optimal - Block Based Algorithms

The focus of block based algorithms is to try and estimate the optimal weighting using blocks of pilot data embedded in the transmitted signal. These methods, though they can converge rapidly to the optimum weightings during training, can get quite complex when additional array elements are present. Another drawback to these methods is that usually block based algorithms do not change their weighting after training. Therefore in the presence of a slowly varying frequency nonselective Rayleigh fading channel, weights are updated only when pilot symbols are received. An example of a block based algorithm is the direct matrix inversion (DMI) algorithm described in [42] and below.

Direct Matrix Inversion (DMI)

DMI is a block based algorithm used to estimate the optimal weight vector with the limited information available for training. This algorithm is an approximation to the optimum solution (Wiener-Hopf) [42] which is given for user n as:

$$\mathbf{w}_{DMI} = \mathbf{R}_{DMI}^{-1}\mathbf{p}_{DMI} \tag{4.7}$$

where $\mathbf{R}_{DMI} = \frac{1}{T_l}\sum_{k=1}^{T_l}(\mathbf{u}(k)\mathbf{u}^H(k))$ is the time average autocorrelation of the received signal vector over the specified training sequence length T_l and $\mathbf{p}_{DMI} = \frac{1}{T_l}\sum_{k=1}^{T_l}(\mathbf{u}(k)d^*(k))$ is the cross-correlation vector between the desired response and the received signal over the same training sequence length. As with block based algorithms, the advantage to DMI is the weight vector is based on finding $[\mathbf{R}]^{-1}$ and $\mathbf{p}$, allowing weights to converge to the desired weight rapidly during training. A limitation of this algorithm is the complexity in calculating $[\mathbf{R}]^{-1}$ and $\mathbf{p}$. In the proposed technique, DMI weights will be calculated for each partial decision subinterval during a training sequence, and held constant throughout the duration of a frame.

4.3.2 Sub-Optimal - Gradient Based Algorithms

A wide variety of gradient algorithms [42–44], which include algorithms such as least mean square (LMS) have been developed over the years. Gradient algorithms are able to converge towards the optimal weight vector given a sufficient amount of samples, by simply updating the current weights based on the error and the previous received signal.

In this thesis when looking at quasi-static Rayleigh fading channels, block and gradient based algorithms will be used. However when looking at slowly varying frequency nonselective Rayleigh fading channels, our focus will be mainly based on gradient algorithms because of their ability to update their weights during small changes in the channel [45]. Thus, the choice of one algorithm over another is determined by these following factors:

Rate of Convergence: The rate of convergence is defined as the number of iterations required before convergence towards a close estimate of the optimal Wiener solutions is found. Faster convergence rates require shorter training sequences for unknown channel characteristics.

Tracking: In non-static environments, it is required that algorithms take into account small changes in a channel. A system that is able adjust for these changes will achieve better performance.

Computational Complexity: For gradient adaptive algorithms, one of the main advantages is the relatively low complexity of the system. This includes such things as number of operations (i.e. addition/subtraction and multiplication/division) and memory allocation (buffer space needed and memory need to store algorithm).

These factors, plus cost, are all important factors in deciding the ideal algorithm. By improving the rate of convergence (i.e. making each step size larger) the system tends towards the optimum weights rapidly. However, this can greatly decrease tracking by changing weightings drastically when only small variations in the channel are present. To improve tracking, a compromise between the rate of convergence and channel variations is needed. To allow for good tracking a system needs to take into account both small and large variations in the channel.

In general, one area causes deterioration in another, designers need to make a thorough analysis in deciding which parameters are most important and design accordingly.

Least Mean Square (LMS)

LMS is a gradient based algorithm used to estimate the optimal weighting vector [43]. To find the LMS weighting vector $\mathbf{w}$, estimates of the mean square error $E\{|e(t_s)|^2\}$ between

the desired and estimated signal, through gradual iterations, to be minimized:

$$\mathcal{J} = E\{|e(t_s)|^2\} \geq \mathcal{J}_{min} \tag{4.8}$$

The algorithm for calculating the weighting vector at time t_s is then:

$$e(t_s) = d(t_s) - \mathbf{w}^H(t_s)\mathbf{u}(t_s) \tag{4.9}$$

$$\mathbf{w}(t_s + 1) = \mathbf{w}(t_s) + \mu\mathbf{u}(t_s)e^*(t_s) \tag{4.10}$$

where μ is the LMS step size that is constrained between $0 < \mu \leq (\text{trace}[\mathbf{R}])^{-1}$, where trace[$\mathbf{R}$] is the average received power [46]. From equation (4.9), there is a direct relationship between μ and e. This relationship for the channel of interest, will be discussed and explored in Chapter 4, where we will find a value for μ to optimize PDV performance.

Although there exist algorithms with faster convergence rates such as recursive least square (RLS) [42], LMS has the advantage of providing low computational complexity and ease of implementation [42], which are important when designing efficient receivers. In this thesis, simulations were done primarily with slowly varying frequency nonselective Rayleigh fading channels. In a static environment block and gradient algorithms have similar performance. However, in a nonstatic environment only recursive algorithms such as LMS offer tracking by simply updating the previous weight. One method to overcome tracking in block based algorithms and improve performance in gradient based algorithms is to introduce pilot symbols [47]. In the section below, we will discuss insertion of pilot symbols and how it will affect performance of the LMS algorithm. The use of pilot symbols can also be extended to include block based algorithms, but will not be discussed.

Pilot Symbol Insertion (PSI)

With the use of a decision-based LMS algorithm, errors can compound drastically when an error is made in a nonstatic environment. Therefore PSI techniques have been discussed in [48, 49], wherein a pilot symbol-assisted system, known pilot symbols, are inserted periodically into the data sequence prior to modulation. The disadvantage of this technique is that additional symbols are required. If we were to transmit the same amount of information without pilot symbols, less bandwidth and energy are needed. Figures 4.1 and 4.2 illustrate how this system is implemented. During transmission of information bits D, a pilot symbol P is inserted every period. The pilot symbol, which contain known information at the receiver, is then sent through an adaptive algorithm and used to update the detector weights.

For our proposed system we simulated the optimized PSI rate for a given LMS step size and constant received power, where the energy per bit is defined as the total received power over P the bit rate R_b, P/R_b (R_b does not count the pilot symbols). The actual channel E_b/N_o is then $P/R_b + 10log(\eta)$, where η is the fraction of channel symbols that are actually bits ($\eta = R_b/R_{(b+p)}$ and $R_{(b+p)}$ is the bit plus pilot rate). Figure 4.3 presents results for a DS-CDMA system employing 4 receive antennas, 6 users, 0.04 LMS step size, and no PDVs. Spreading sequence and energy to noise ratios were adjusted such that the same data sequence, without pilot symbols contains the same bandwidth and energy as data using PSI. It is seen that the BER decreases initially as the PSI rate increases, improving the accuracy of the weights. At higher PSI rates, however, the performance worsens as the effective SNR becomes too low to support an adequate BER.

4.4 Summary

In this chapter we discussed the use different algorithms to compute the weighting vector for the PDV technique. To further improve the performance of the system, pilot symbols were inserted periodically to help track Rayleigh fading channels. In the next chapter of this thesis, we will use a PSI rate of 16 found in Figure 4.3 to find the performance of the PDV technique.

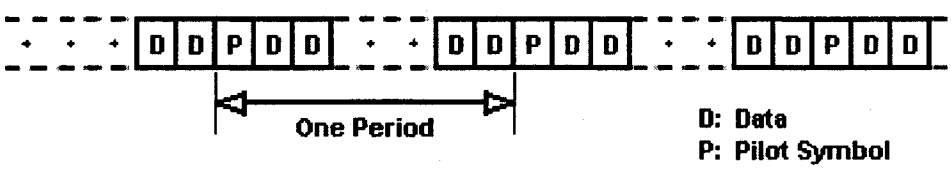

Figure 4.1: Frame structure.

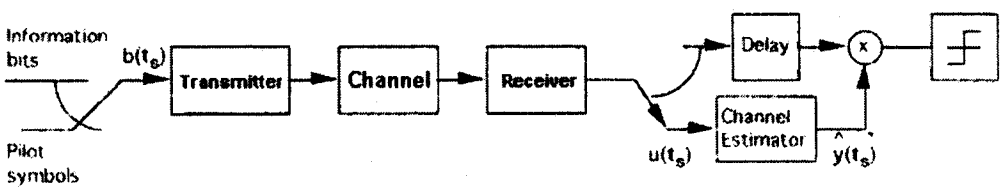

Figure 4.2: Block diagram of a pilot symbol assisted communication system.

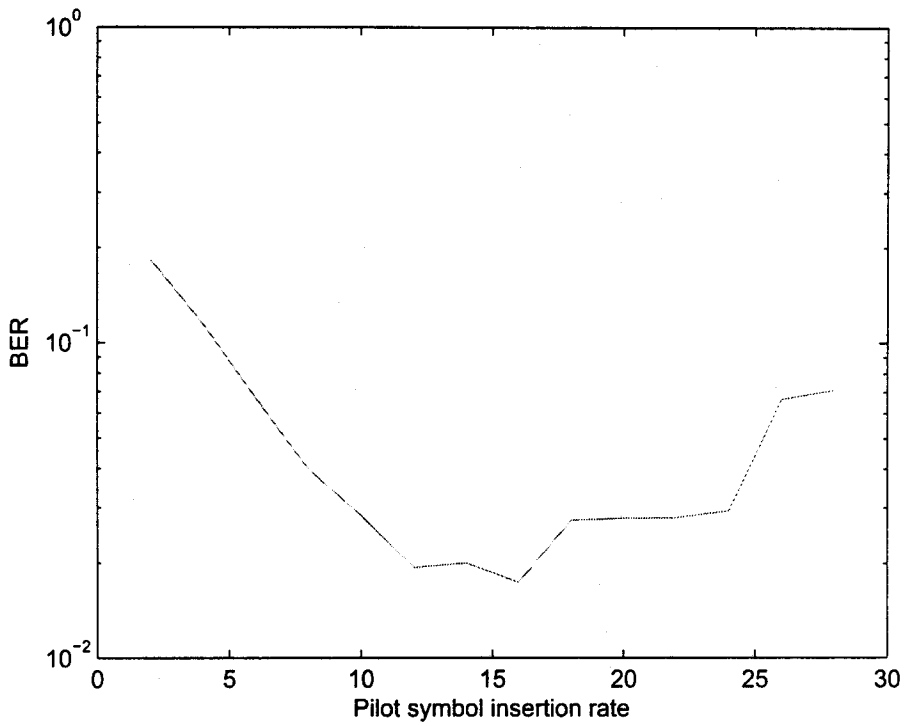

Figure 4.3: BER of pilot assisted DS/CDMA technique using a LMS step size 0.04, E_b/N_o 20dB, 6 users, 4 receive antennas at a normalized Doppler rate of 0.01.

Chapter 5

Simulation Results

5.1 Simulation Parameters

All simulations have been performed using Matlab. Here, we provide the assumptions and conditions used in the simulation models which are as follows:

1. We are considering a symbol synchronous N user DS-CDMA system employing BPSK modulation;
2. All thermal noise is assumed to be AWGN;
3. All users' signals are transmitted at the same bit rate;
4. Channels are assumed to be linear;
5. All user's signal are received with equal power (perfect power control assumed for simplicity);
6. Techniques used to find weighting vector will include initial training followed by decision-feeback LMS (described in Chapter 3);
7. The training length used is 2000 bits (used to allow adequate convergence of LMS); and
8. Including training sequences we simulated 100 trials with 16000 bits per trial. In every trial we regenerated the channel gain and spreading sequences. The results of all the trials are then averaged to find performance results.

In the simulations, direct modeling of the spreading and despreading will be computationally inefficient. Therefore simulations have been implemented using equation (2.3) to directly model the decision variables at the receiver. To find the cross-correlation between each user, spreading sequences were generated for each and the correlation between them are calculated.

5.2 Simulation Conditions

The main objective of this thesis is to analyze the performance of the PDV technique. To perform a thorough analysis, it would be necessary to compare the performance in various scenarios. Simulations will be performed on these various types of channels:

1. AWGN channel - 1 transmit antenna, with 1 receiver antenna where each channel is assumed to have a gain of 1.
2. Quasi-static Rayleigh fading channel - 4 transmit antennas, with 4 receiver antennas where fading over each link is assumed to be independent.
3. Slowly varying frequency nonselective Rayleigh fading channel - 4 transmit antennas, with 4 receiver antennas where fading over each link is assumed to be independent.

For both the AWGN and quasi-static Rayleigh fading channels we only look at varying E_b/N_o. Our main focus will be on the slowly varying frequency nonselective Rayleigh fading channel, where we will perform PDV analysis over the following parameters:

1. Variable E_b/N_o
2. Variable spreading factors
3. Variable number of transmitting users
4. Variable number of receiving antennas.

5.3 AWGN Channel

To begin our PDV analysis, simulations were first carried out in AWGN channel to duplicate the results in [3]. For our simulations we assumed the AWGN channel has constant gain of 1 with no phase error and different spreading sequences. Also LMS was used during training

sequences followed by decision feedback LMS after training. Shown in Figure 5.1 is the simulated result for BER performance using the PDV system with 3 users and a spreading factor of 20 with LMS weighting. The results show that using 5 PDVs provides improvements relative to the conventional system where a single decision variable is used. The plot shown in Figure 5.1 is the same as the one provided in [3], thereby confirming our model for the use of the PDV technique.

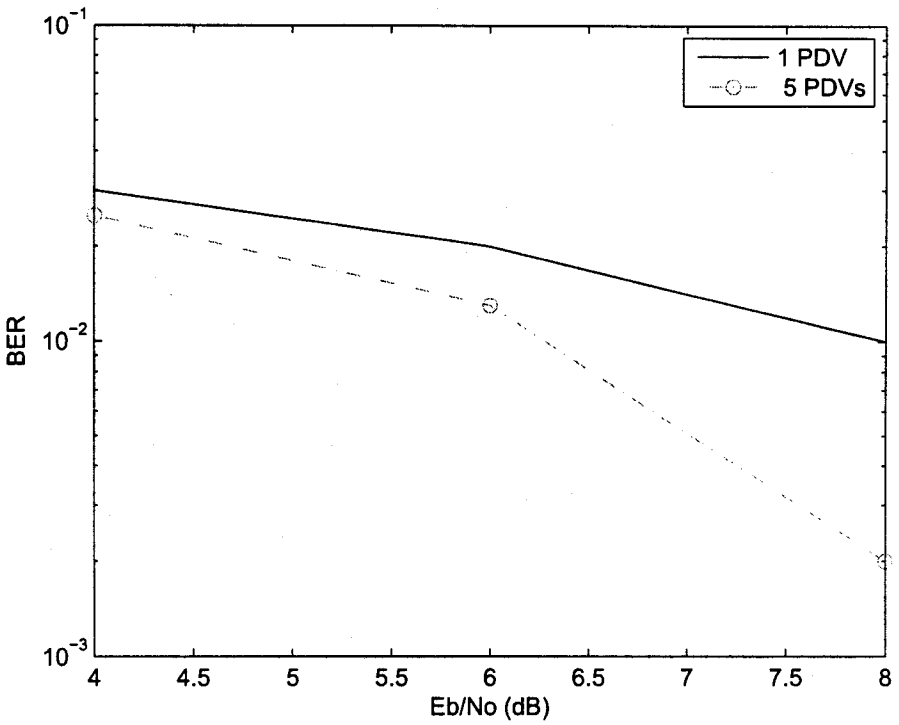

Figure 5.1: Bit error rate performance of a 3 user synchronous DS-CDMA system in an AWGN channel with SF = 20 and LMS weighting.

5.4 Quasi-Static Rayleigh Fading Channel

In the following sections we will focus on the analysis of the PDV detector in the Rayleigh fading channel described in Chapter 2. Before implementing the slowly varying frequency nonselective Rayleigh fading channel, simulations were undertaken for a quasi-static Rayleigh

fading channel where we assumed that the fading coefficients are constant over the duration of a trial but independently generated on different trials. In practice, wireless channels vary in time because of movement in the transmitter and/or receiver or the surrounding environment. With this use of a quasi-static Rayleigh fading channel, we assume that the channel varies slowly enough that its statistics do not change over the transmission interval. Figure 5.2 provides the results for the case of a quasi-static Rayleigh fading channel with 6 users, 4 receive antennas and a spreading factor of 20.

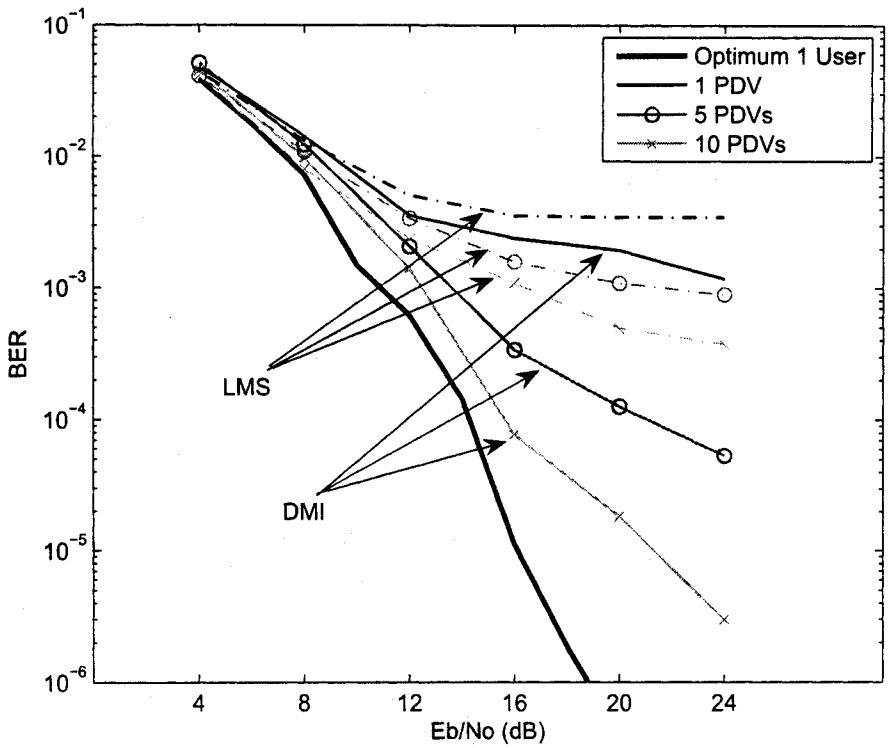

Figure 5.2: Bit error rate performance of 6 user synchronous, 4 receive antennas synchronous DS-CDMA system with a SF = 20 in a quasi-static Rayleigh fading channel.

Figure 5.2 illustrates the comparisons between the PDV and the conventional technique in a quasi-static Rayleigh fading channel. For both the LMS and DMI case, a 2000 bit training sequence length was used to find the weighting vector which were then applied to each PDV over the subsequent 14000 information bits. From Figure 5.2 we see that even though both LMS and DMI should provide good estimates to the Wiener solution weights,

the BER performance of DMI is better than LMS. This difference is attributed to DMI weights being time-averaged over a the entire training sequence to approximate the Wiener solution. When using decision based LMS weights, since it is a gradient algorithm, excess error always exists. Figure 5.4 shows the convergence and tracking error of LMS over the duration of a trial. Over time LMS slowly converges, but excess error is still present due to inappropriate step sizes, which will be addressed later in this Chapter. However, LMS will be implemented for its ability to track and for its low complexity, which will be important when communicating over slowly varying frequency nonselective Rayleigh fading channels. Figure 5.2 also presents the BER performance for a 1 user, 4 receive antennas system with a spreading factor of 20 (labeled optimum BPSK); this will be considered our lower bound for simulations because it is an optimum case where no MAI is present. From the figure as the number of PDVs increases, the BER performance gradually approaches the Wiener Solutions.

5.5 Slowly Varying Frequency Nonselective Rayleigh Fading Channel

Figure 5.2 showed the performance over a quasi-static Rayleigh channel. In a more realistic cases, the fading process is time varying. In this section we simulate PDVs in a slowly varying frequency nonselective Rayleigh fading channel with a normalized Doppler spread of $f_dT = 0.01$. Each simulation consisted of averaging results obtained from 100 independent slowly varying frequency nonselective Rayleigh fading channels. For each trial, training sequences of 2000 bits were used to find LMS weights with LMS step size $\mu = 0.04$ as discussed below. While transmitting the subsequent 14000 information bits, decision feedback (DFB) is used for tracking purposes. To prevent an error event from causing catastrophic errors, pilot symbols were also inserted every 16 bits for LMS tracking. BER is then calculated using only the information symbols.

Figure 5.3 shows results obtained using a normalized Doppler spread $f_dT = 0.01$. From the figure at low $E_b/N_o < 7$dB, using PDVs does not provide an advantage, while at $E_b/N_o = 7$dB we see improvements using 2 PDVs. With an $E_b/N_o \geq 16$dB, the advantage of PDVs is evident where 2 PDVs and 5 PDVs outperform using 1 PDV. When the number of PDVs is increased to 10 the same trend occurs, providing improvements only at higher SNR ($E_b/N_o \geq 24$dB). When using more PDVs, the noise component in each decision variable is greater then no decision variables, by using more PDVs at lower E_b/N_o minimizing the MSE of the

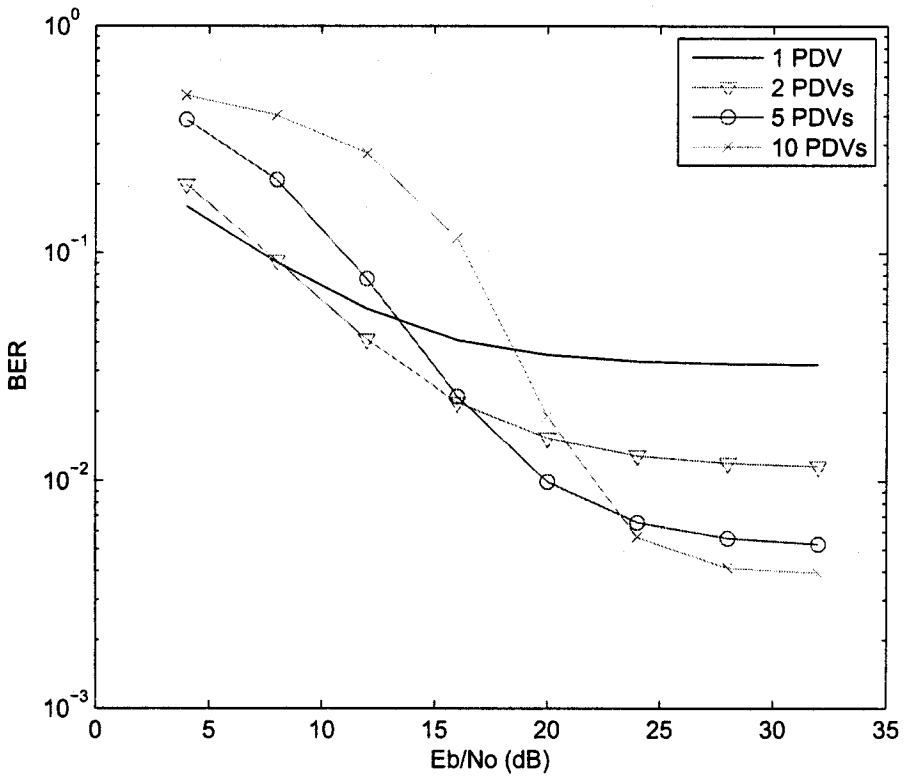

Figure 5.3: Bit error rate performance of 6 user synchronous, 4 receive antennas synchronous DS-CDMA system with a SF = 20 in a slowly varying frequency nonselective Rayleigh fading channel with normalized Doppler shift of 0.01.

signal PDVs does not eliminate the additional noise, showing lower performance. As we increase the the E_b/N_o using LMS is able to better eliminate noise and MAI. In general as we increase the number of PDVs the error floor decreases but the optimum operating SNR increases as well. Using 10 PDVs we can see an error floor improvement of approximately 1 order of magnitude relative to using a single decision variable.

5.5.1 LMS Investigation

As discussed in Chapter 3 we know that LMS uses a gradient method to slowly converge towards the optimized weighting vector given that the channel does not change significantly over the desired time interval. In a CDMA system however, where MAI plays a major role in

the received signal, PDVs change. The step size parameter μ defines the rate of response to changes. Figures 5.4 and 5.5 show the difference between using two different LMS step sizes of 0.01 and 0.04. Figures 5.4 and 5.5 show for a 6 user, 4 receive antennas system with a

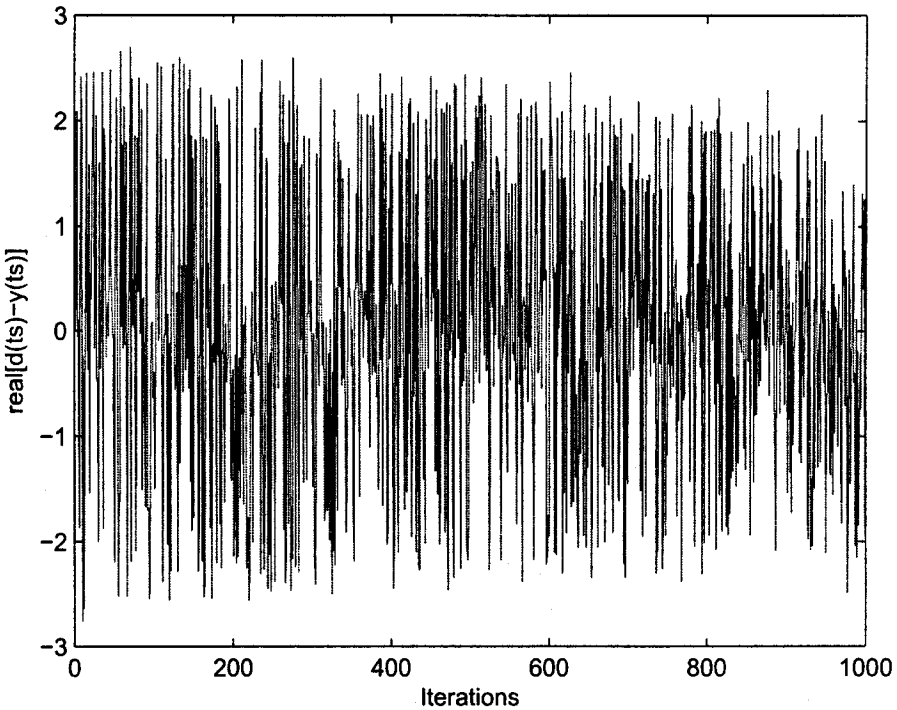

Figure 5.4: Difference between optimum weights and LMS weights with a step size of 0.01 in a 6 user, 4 receive antennas system with SF = 20 and 5 PDVs.

spreading factor of 20 and 10 PDVs, using different LMS step sizes can alter the tracking of the LMS algorithm. Figure 5.4 illustrates the effect of a step size smaller than the optimized. By updating the weights with small step sizes, the difference between the current weight and next weight are relatively the same and will not alter the BER performance. However, when using a step size larger then the optimized, the convergence of the weights are rapid but never converge closely to the optimum weights.

By investigating these results it was found that given different LMS step sizes, the performance of using PDVs can be affected. As stated in Chapter 3, for a given set of partial decision variables, the decision $\mathbf{y}$ can be computed using a weighted sum of each variable to

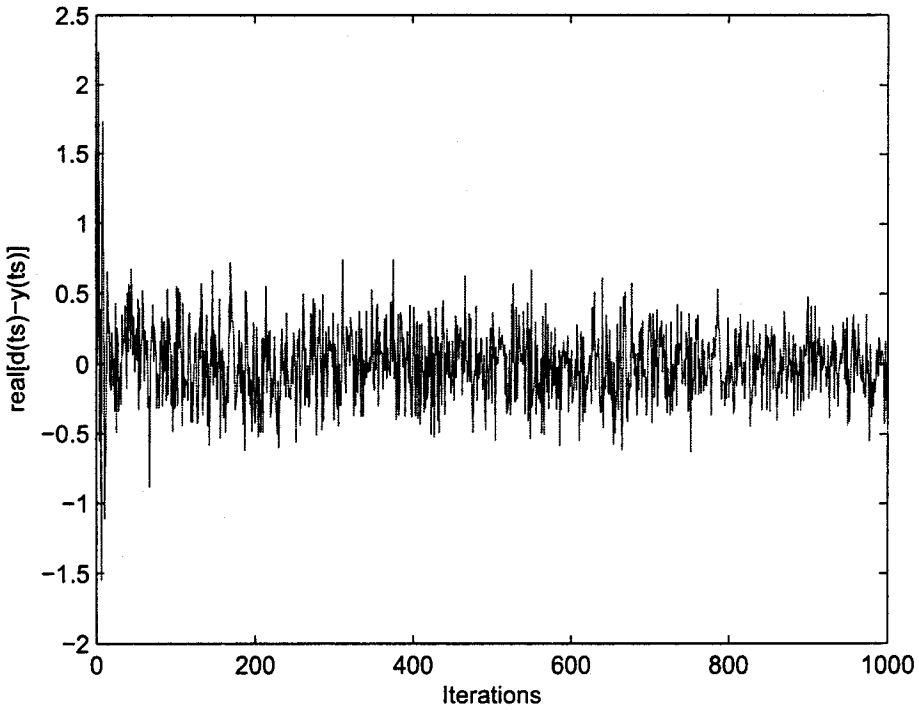

Figure 5.5: Difference between optimum weights and LMS weights with a step size of 0.04 in a 6 user, 4 receive antennas system with SF = 20 and 5 PDVs.

maximize the signal to interference plus noise ratio given by:

$$\mathbf{y}_n = \sum_{k=1}^{N_r} \sum_{x=1}^{X} w^*_{x,n,k} u_{x,n,k} \tag{5.1}$$

where $w_{x,n,k}$ is the xth tap weight of the kth antenna of user n as shown in Chapter 4. Therefore by increasing the number of decision variables, the smaller each individual weight contribution will be. Figure 5.6 compares various step sizes with 1, 2, 5 and 10 PDVs. For a 6 user system at 25dB with a spreading factor of 20, different step sizes were computed and BER performance was calculated. For 1, 2, 5 and 10 PDVs the optimum step sizes are approximately 0.4, 0.1, 0.04, and 0.03 respectively. When using adaptive weighting the weight of each PDV is inversely related to the number of PDVs. Therefore the optimum step size should not be too small such that it does not converge after training or too large such that the step size will drastically change each weighting. We validate these results by

looking at maximum step size for stability, using 5 PDVs $[\{\text{trace}(\mathbf{R})\}]^{-1}$ is slightly greater than the optimum step size found in Figure 5.6. Results also showed that given the use of more PDVs, the optimized LMS step size is smaller.

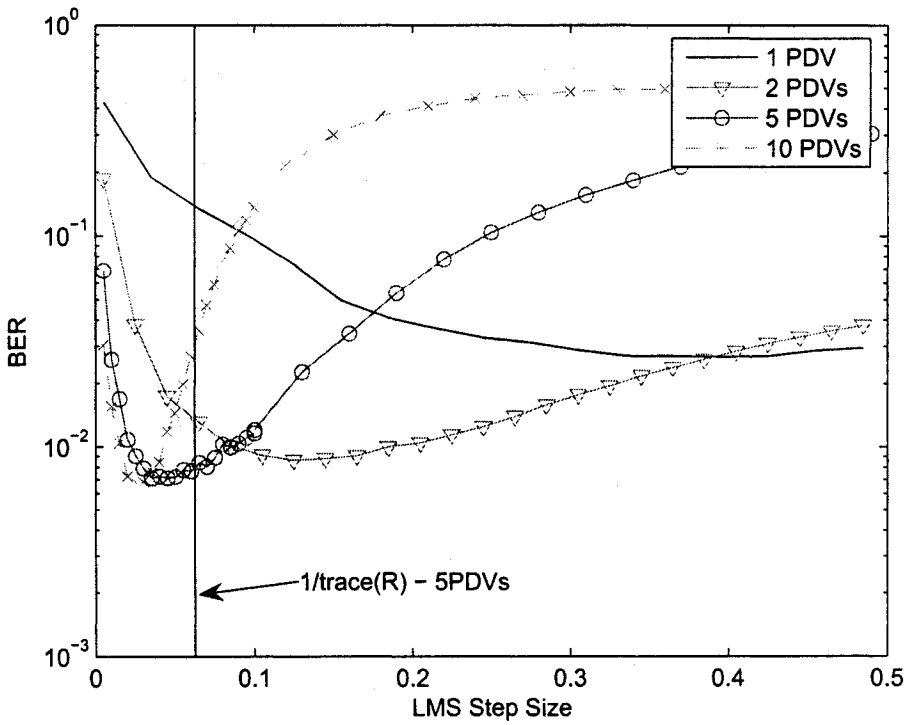

Figure 5.6: LMS step size in a 6 user, 4 receive antennas system with SF = 20 at 25dB.

Varying f_dT

In a realistic environment mobile transmitters do not travel at a constant speed, which in turn alters the normalized Doppler rate. Different normalized Doppler rates are presented in Figure 5.7 with the same parameters as those in Figure 5.6 and their optimized LMS step size is computed. From Figure 5.7 we see that a different Doppler rates require different optimized LMS step sizes. One thing to note is that by varying the step size, at lower Doppler rates, the change in BER is more apparent and one should adjust the step sizes according to the lowest Doppler rate.

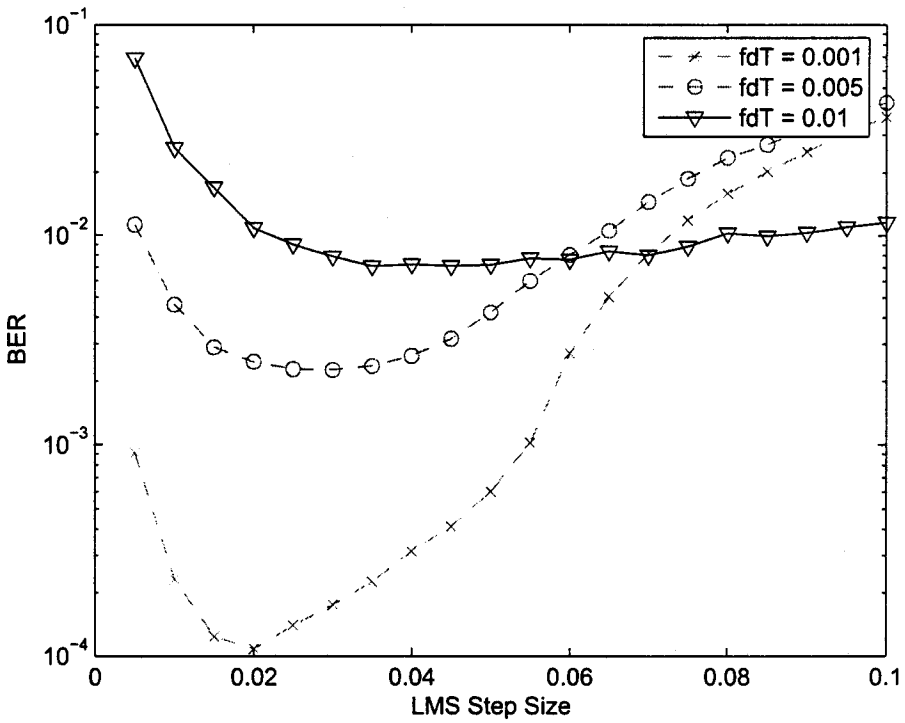

Figure 5.7: Different LMS step sizes and f_dT in a 6 user, 4 receive antennas system with SF = 20 and 5 PDVs at 25dB.

5.5.2 Parameter Investigation - 25dB

In this section, different parameters were analyzed with the aim of optimizing the performance of the PDV technique. The performance was evaluated by fixing the SNR of the system to be 25dB with a normalized Doppler spread of 0.01. The different parameters varied are: spreading factor, number of transmitting users, and number of receive antennas. Since at 25dB the performance of 10 PDVs is similar to using 5 PDV, we will not include 10 PDVs in our simulations.

Variable Number of Users

Figure 5.8 presents the BER performance while increasing the number of users with a spreading factor of 20, 4 receive antennas and weightings with optimized LMS step sizes. As expected, when the number of users increases the BER performance worsens. The advantage

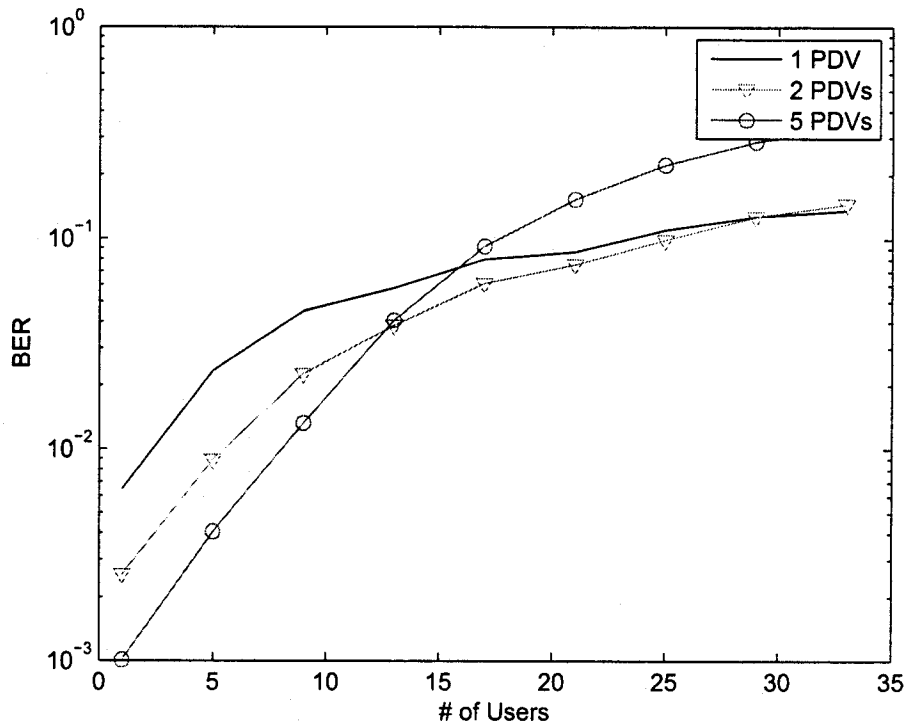

Figure 5.8: Impact of varying the number of users with 4 receive antennas, a SF = 20 and optimized LMS step sizes at 25dB.

of the PDV technique is seen when we slowly increase the number of users in a system, for a moderately loaded system of 5-10 users or 0.25-0.5bps/Hz, the use of PDVs provides the most gain. However, when we keep increasing the number of users using additional PDVs shows worse performance. Due to the central limit theorem, as we increase the number of transmitting users the distribution of each subinterval tends towards Gaussian. Thus the SINR of the decision variables on each subinterval tends towards a Gaussian random variable and equal weighting becomes optimum. Though we expect the PDV technique to tend towards that of no PDVs when increasing the number of users, additional error is introduced by having the increased number of LMS weights. For the optimum case of 1 user where no MAI is present, we would expect that using multiple PDVs would converge to using 1 PDV. Though the weights do not have to cancel interference caused by other users, using different weightings minimizes errors caused by channel phase.

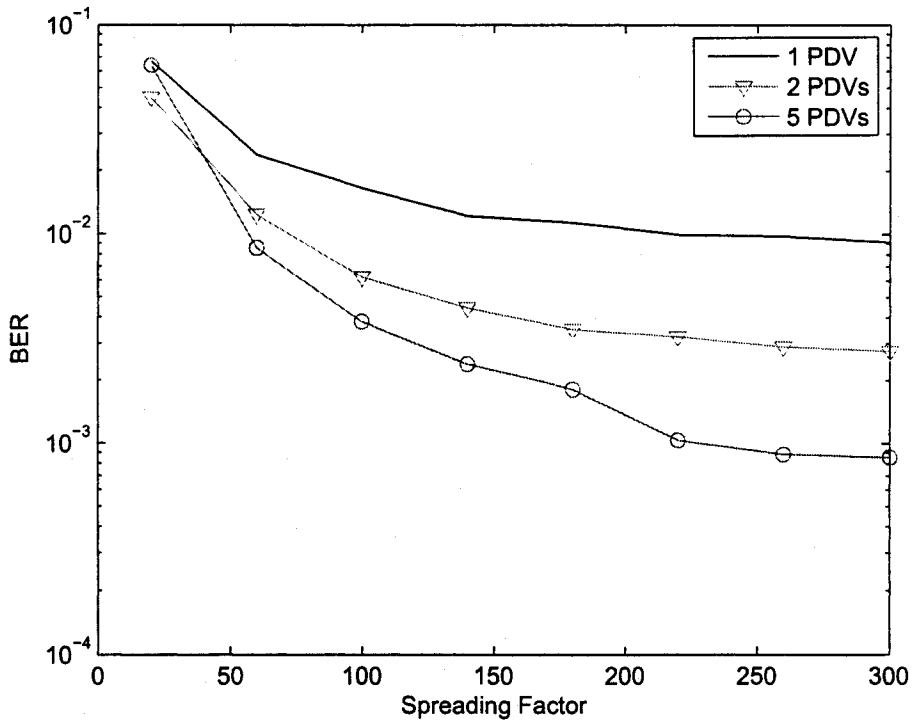

Figure 5.9: Impact of varying the spreading factor with 15 users, 4 receive antennas and optimized LMS step sizes at 25dB.

Variable Number of Spreading Factors

In Figure 5.9 using PDVs for a 15 user, 4 receive antenna system and implemented using optimized LMS step sizes, different spreading sequences lengths were simulated. With 15 users and a spreading factor of 20 (0.75bps/Hz) the system is heavily loaded, and the use of PDVs does not show much improvement. But as we increase the length of the spreading factor, lowering the load of the system, the PDV technique shows better BER performance. An important thing to note in this figure is the performance increases logarithmically, as we increase the spreading factor we should expect our BER performances to converge to the optimum BER.

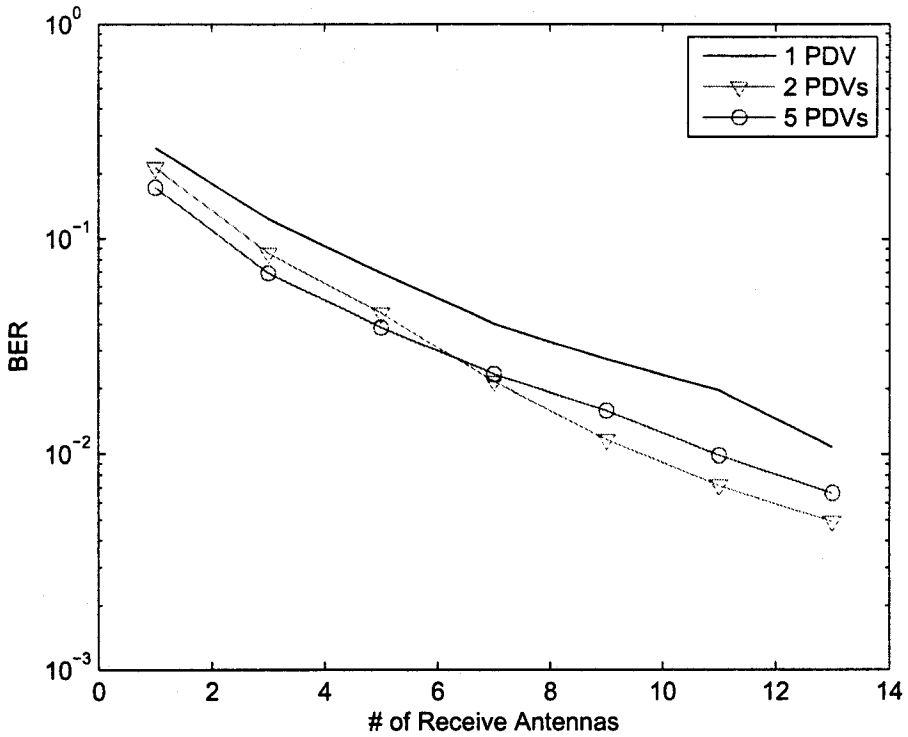

Figure 5.10: Impact of varying the number of receive antennas with 15 users, a SF = 20 and optimized LMS step sizes at 25dB.

Variable Number of Receive Antennas

The impact of additional receive antennas on the system is shown in Figure 5.10. From the figure, we can identify that the PDV technique can provide BER improvements given a specific number of antennas. In the case of Figure 5.10 given a system with 15 users and a spreading factor of 20, no significant gain is achieved by increasing the number of receive antennas. One thing to note is when increasing the number of receive antennas, the number of weights increases while $[\text{trace}(\mathbf{R})]^{-1}$ decreases, making each individual weight smaller. With smaller weights the error associated with changing μ drastically increases, affecting overall performance of the system. When using 6 receive antennas the performance of using 5 PDVs drops below that of using 2 PDVs, which can be attributed to the errors caused by μ.

5.5.3 Parameter Investigation - 15dB

The above section investigated parameters at a E_b/N_o of 25dB which is not practical for cellular communication. This section will focus on Figure 5.3 at E_b/N_o = 15dB, where performance would be similar to that of cellular communication. Figures 5.11 - 5.13 are similar to the plots above, reiterating observations obtained previously. One thing to note is that the performance gains found at 15dB in Figures 5.11 - 5.13 are not as significant and the use of 2 PDVs outperforms 5 PDVs. This informs us that it is necessary to use a smaller number of PDVs as we decrease E_b/N_o.

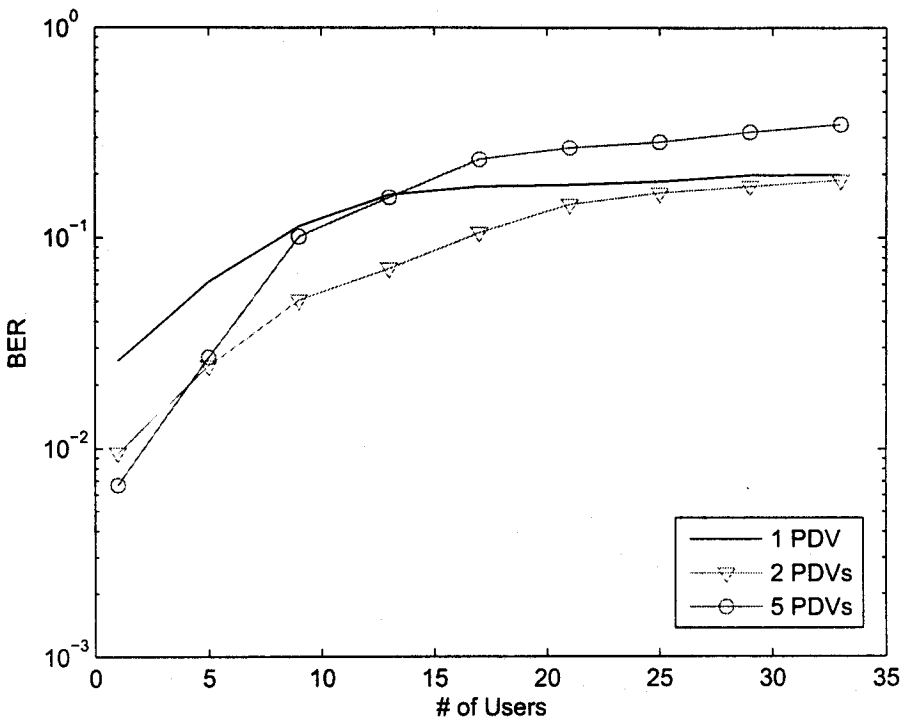

Figure 5.11: Impact of varying the number of users with 4 receive antennas, a SF = 20 and optimized LMS step sizes at 15dB.

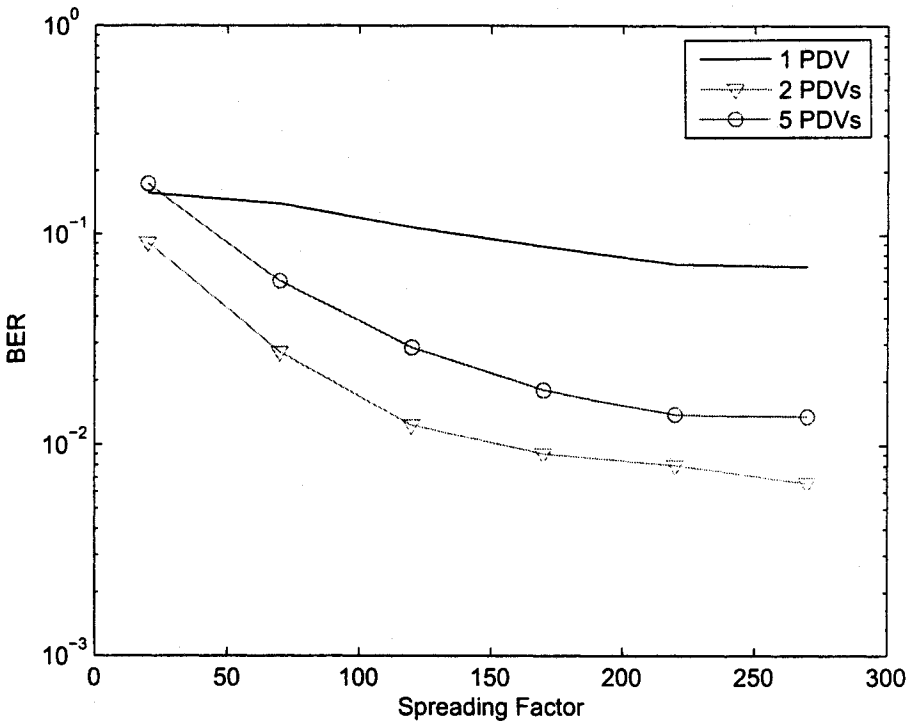

Figure 5.12: Impact of varying the spreading factor with 15 users, 4 receive antennas and optimized LMS step sizes at 15dB.

5.6 Measured Channel Data

Measured channel data in a wireless environment presented in Chapter 2 contained information for a 4 transmit and 4 receive antenna system. This system can be extended to a multiuser CDMA system by considering each transmit antenna as a distinct user, creating a 4 user CDMA system with 4 antennas at the receiver. Figure 5.14 shows the frequency response of the channel over 1 second. The maximum Doppler shift of this channel was estimated to be 45Hz, when multiplied by the sampling rate the normalized Doppler frequency is $f_d T_s = 0.18$. To compare results for both cases a similar normalized Doppler frequency needs to be used. In this thesis we increased the sampling rate of the measured signal using interpolation by a factor of 18 to achieve a normalized Doppler spread of 0.01.

Figures 5.15 and 5.16 compare the performance of a Rayleigh flat fading channel and measured channel data with 4 users, 4 receive antennas, spreading sequence of 20, LMS

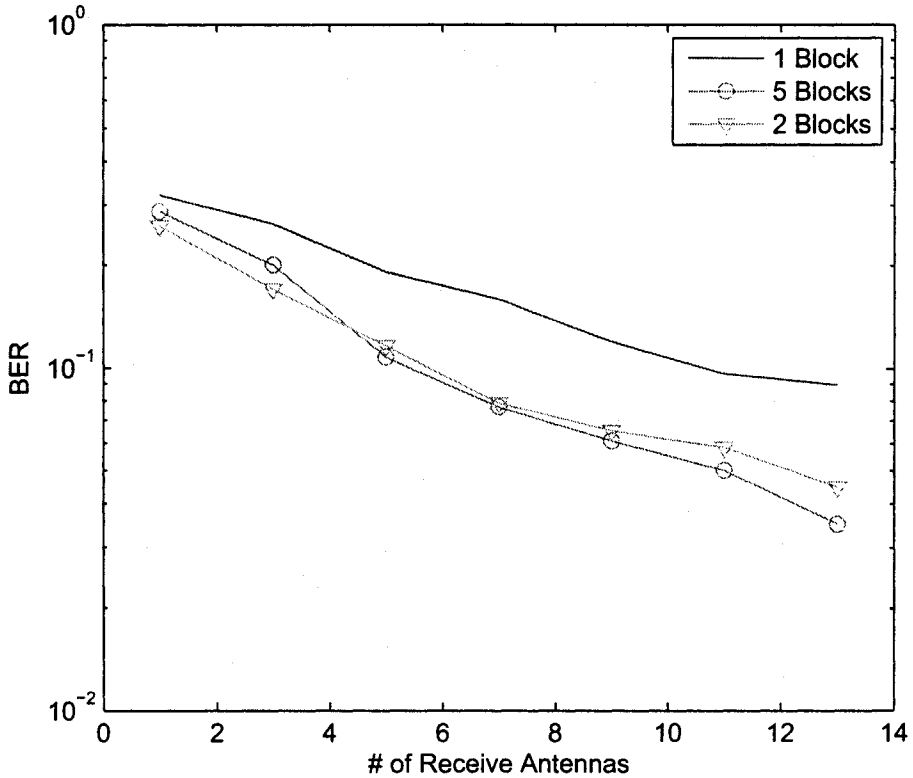

Figure 5.13: Impact of varying the number of receive antennas with 15 users, a SF = 20 and optimized LMS step sizes at 25dB.

weighting and a normalized Doppler frequency of 0.01.

When using measured channel data, the BER performance worsens when compared to the simulated flat fading channel. This loss is expected due to the correlation in measured data. A significant difference between the two sets of data is the point at which the PDV technique outperforms the conventional method. For the given set of measured channels, the intersection is decreased by 6dB, in favour of the PDV technique. This difference can also be attributed to the correlation of the channels. Since the PDV technique tries to minimize SINR, at an E_b/N_o of 12dB interference caused by correlation becomes dominant over noise for 5 PDVs.

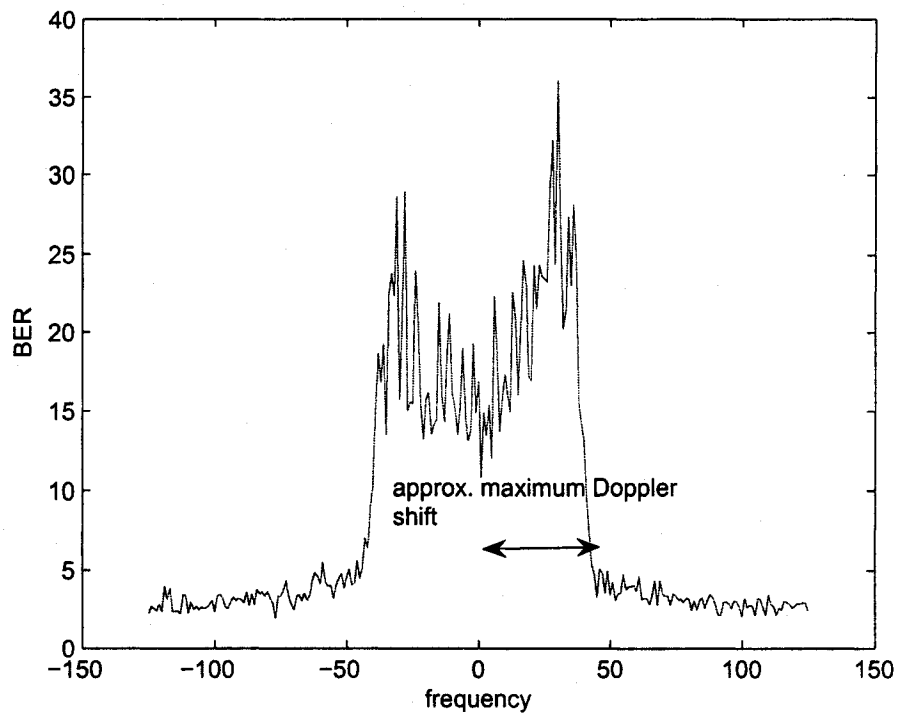

Figure 5.14: Frequency spectrum of measured channel data.

5.7 Complexity Analysis

The goal of using PDVs is to reduce the number of computations necessary for MAI cancelation. Computational complexity is very important for implementation because detectors that require complex algorithms need more powerful devices. The computational complexity per bit for a given multiuser detector is obtained by performing an analysis similar to [50]. In this thesis we will calculate the complexity of PDVs in terms of: number of users N, the number of signaling interval X, the spreading factor K, and the number of receive antennas N_r.

Consider a N user DS-CDMA system employing PDVs. Over one signaling interval, each user transmits 1 bit. At the receiver all signals received in sub-intervals are combined with desired weighting and a decision is made. Assuming that complex additions and multiplications are performed, PDV weighting requires two multiplications and three additions for each sub-interval. During one signaling interval, the receiver for one user detects X subin-

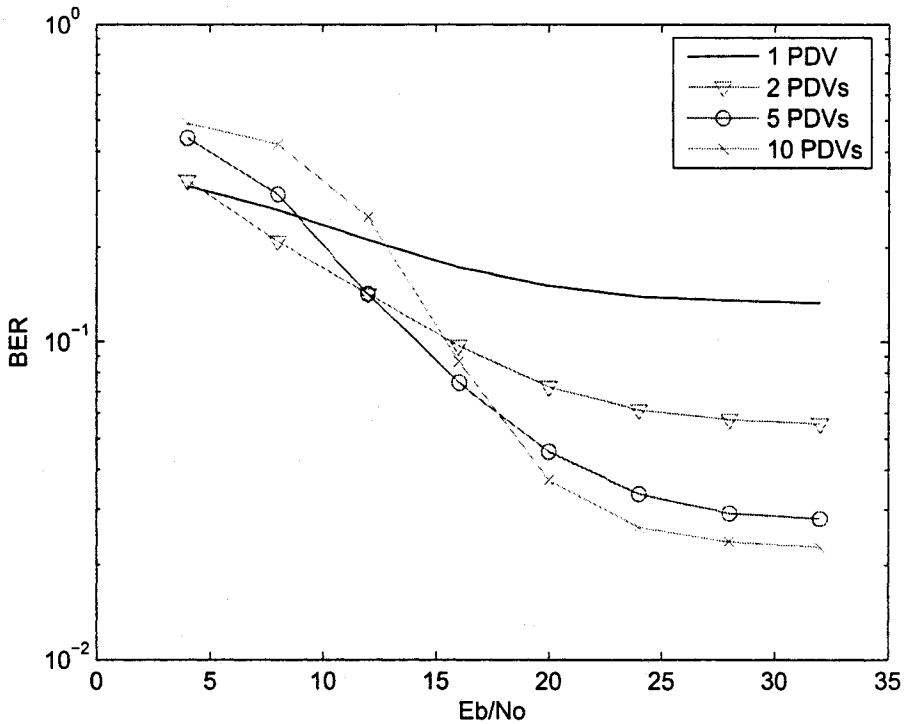

Figure 5.15: Bit error rate performance of 4 user synchronous, 4 receive antennas synchronous DS-CDMA system with a SF = 20 with measured channel data and a normalized Doppler spread of 0.01.

tervals over N_r antennas. Therefore over one signaling interval, the receiver must perform $5KXN_r + (KXN_r - 1)$ operations. Then for N user detection the complexity increases to $5NKXN_r + 5(NKXN_r - 1)$. Comparing this result to the case when no PDVs are used, complexity increases proportional to X. When comparing this algorithm to a decorrelating detector, even through BER performance is better (shown in Figure 5.17), has complexity N^3, the PDV technique requires significantly less complexity while maintaining good BER performance.

5.8 Summary

In the case of a quasi-static Rayleigh fading channel, results obtained showed the PDV technique had significantly better performance than the conventional detector with multiple

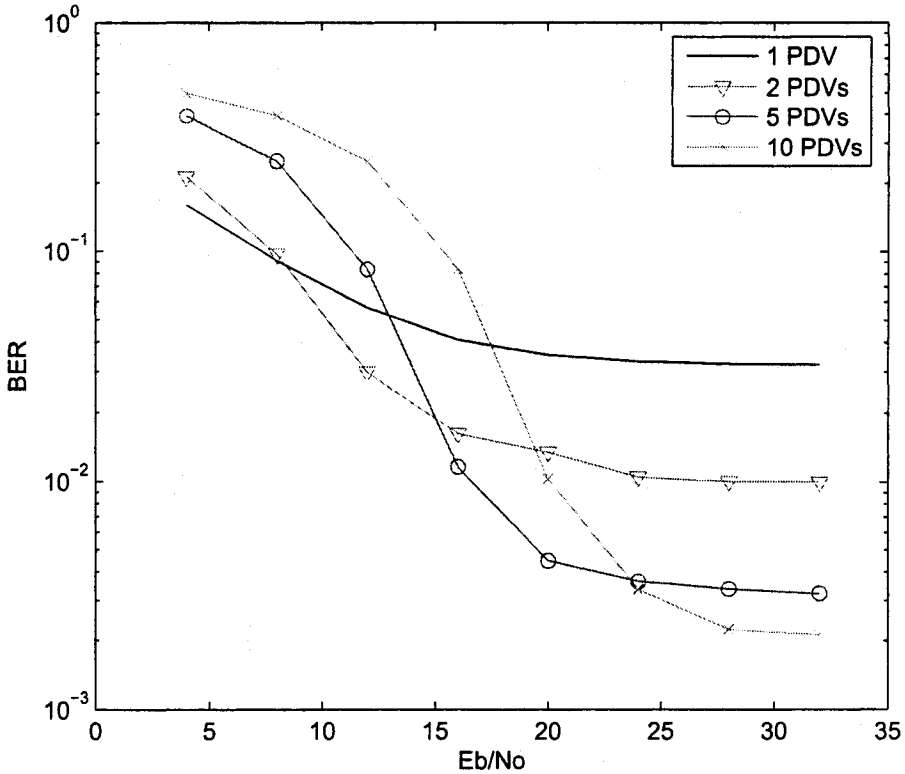

Figure 5.16: Bit error rate performance of 4 user synchronous, 4 receive antennas synchronous DS-CDMA system with a SF = 20 in a slowly varying frequency nonselective Rayleigh fading channel and normalized Doppler spread of 0.01.

receive antennas. In the slowly varying frequency nonselective Rayleigh fading channel however, the gains were not as significant. Even though we have promising results for $E_b/N_o \geq$ 16dB, at lower E_b/N_o, using 5 PDVs does not provide a significant advantage over the conventional technique. In the case of 2 PDVs, performance is not as good as 5 PDVs but it will provide gains at $E_b/N_o \geq$ 8dB. When using the PDV technique, increasing both the received antennas, spreading factor, and number of transmitting users we can see gradual increases in performance of using PDVs. In Figure 5.3 we are able to note that at lower SNR values ($E_b/N_o \leq$ 15dB), using 5 PDVs does not perform as well as using 2 PDVs. The most important result obtained in this section is when simulations were performed in measured channel data. When using measured channels, the intersection between using 1 PDV and 5

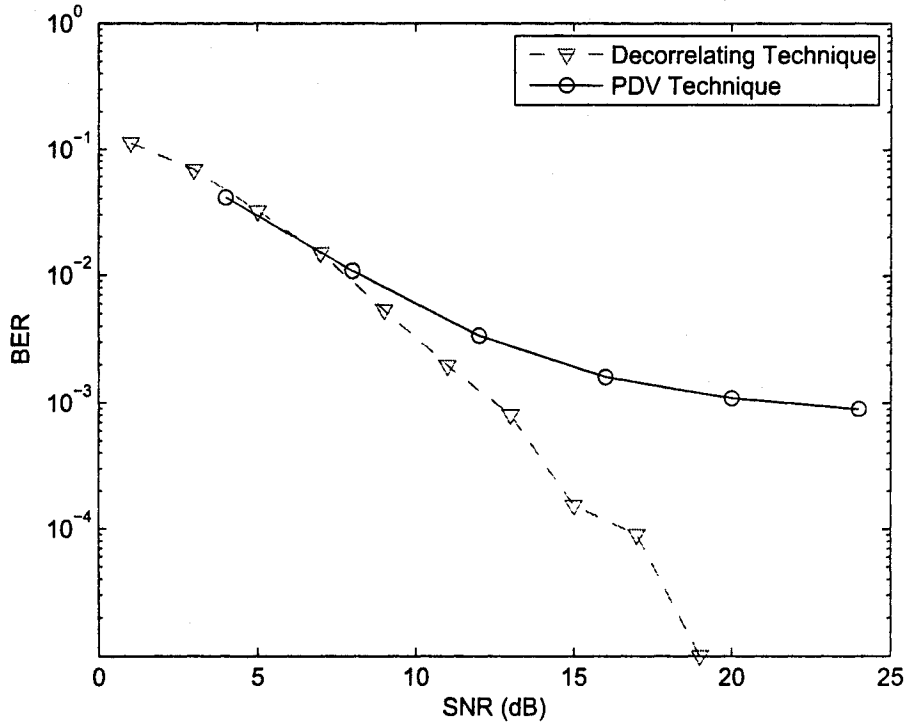

Figure 5.17: Bit error rate performance comparison of 6 user, 4 receive antennas synchronous DS-CDMA system with SF = 20 and quasi-static Rayleigh fading.

PDVs is decreased by 6dB, in favour of the PDV technique. These performance parameters however, are dependent on the optimized LMS step size. If a proper step size is not used, performance can degrade significantly. One method to do this can include switching from a lower number of PDVs to a higher number. For the system described in Figure 5.3 we can switch between 1 to 2 to 5 and to 10 PDVs at E_b/N_o of 8, 16, and 24 respectively.

Overall the use of PDVs with LMS detection can provide additional gain, with relatively low increase in complexity. This additional gain, produced at a higher E_b/N_o, can provide an uncoded BER less than 5×10^{-2}.

Chapter 6

PDVs for Multiple Input Multiple Output (MIMO)-CDMA Systems

6.1 Introduction

It has been recognized that the use of multiple transmit and receive antennas increases diversity over traditional single input multiple output systems (SIMO). Extending this concept to a CDMA environment, SCDMA can be used at the expense of introducing MAI. Similar to conventional CDMA systems, MAI reduction is important for SCDMA systems.

In this chapter of the thesis we extend work in chapter 4 to create a low complexity system that utilizes PDVs in SCDMA systems.

6.2 Space-Time MIMO Detection

Two main techniques already proposed to exploit MIMO systems are: space-time block (STBC) codes, introducing redundancy across multiple antennas [21] and spatial multiplexing (SM), which generates multiple symbols and transmits them over different antenna elements [22]. In this section we will be mainly looking at STBC described below.

Space-Time Block Codes (STBC)

Space-time codes (STC) were first introduced in [21] to improve system performance in fading environments. By employing multiple antennas at both the transmitter and receiver, systems can achieve transmit and receive diversity.

STBC (which is a class of STC) distribute data across N_t antennas and T_i time intervals. Usually the easiest representation of STBC is in matrix form. In this form, each row represents a specific signaling interval and each column represents a specific antenna:

$$\mathbf{G} = \begin{pmatrix} g_{1,1} & g_{1,2} & \cdots & g_{1,N_t} \\ g_{2,1} & g_{2,2} & \cdots & g_{2,N_t} \\ \vdots & \vdots & \ddots & \cdots \\ g_{T_i,1} & g_{T_i,2} & \cdots & g_{T_i,N_t} \end{pmatrix} \tag{6.1}$$

where g_{t_i,n_t} is the modulated signal to be transmitted on antenna n_t and signaling interval t_i.

An important parameter for STBC is the code rate (which measures how many symbols per signaling interval it transmits over one block) [21]. If we were to transmit X_s symbols, then the code rate is:

$$rate = \frac{X_s}{T_i} \tag{6.2}$$

Unfortunately there are only limited codes that can achieve full rate (Rate = 1). One of the first papers introducing STBC was made by Alamouti [29] in 1998, proposing a simple 2×2 block code that achieves full rate (rate = 1). Higher order STBCs were introduced by Tarokh [51, 52].

6.3 System Model

To extend the existing system described in chapter 4, we introduce using the PDV technique for SCDMA system. To exploit the code diversity available in a CDMA system, intervals can be divided into multiple detection subinterval at the receiver, and PDVs generated for each. These PDVs are then weighted according to their respective SINR's and combined, improving SINR and hence BER.

A baseband model of the proposed transmit system is presented in Figure 6.1. From the figure the input data sequence of length L_b is converted to a parallel data vector, which is spread using a space-time coding sequence (STCS). Specifically by employing a coding block $\mathbf{G}$, user n transmits information bits of length L_b that are spread using sequences of length K and transmitted over T_i adjacent symbol intervals using N_t antenna elements.

The baseband model of the received signal is shown in Figure 6.2, where the on-air signal for user n can then be written as the $T_i \times N_t$ matrix $\mathbf{G}_n$ and the total received space-time

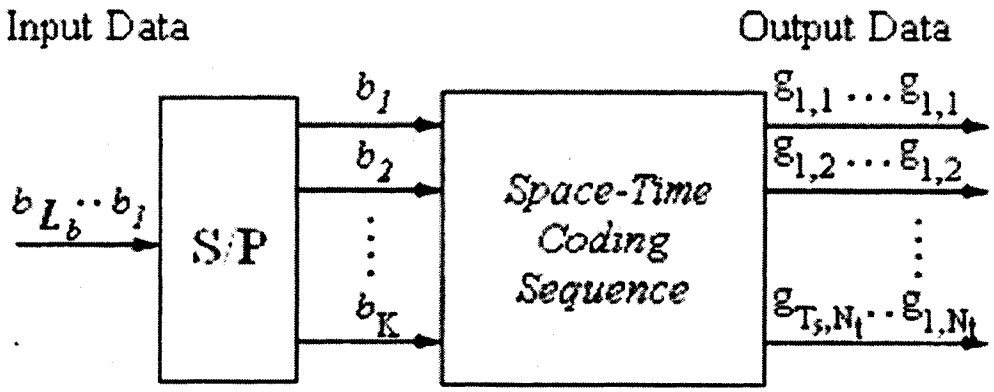

Figure 6.1: Transmitting block diagram of the SCDMA system using PDVs.

signal without any interfering users is given by the $T_i \times N_r$ matrix (assuming $X = N_t$):

$$\begin{bmatrix} r_{1,1} & r_{1,2} & \cdots & r_{1,N_r} \\ r_{2,1} & r_{2,2} & \cdots & r_{2,N_r} \\ \vdots & \vdots & \ddots & \vdots \\ r_{T_i,1} & r_{T_i,2} & \cdots & r_{T_i,N_r} \end{bmatrix} = \begin{bmatrix} g_{1,1} & g_{1,2} & \cdots & g_{1,N_t} \\ g_{2,1} & g_{2,2} & \cdots & g_{2,N_t} \\ \vdots & \vdots & \ddots & \vdots \\ g_{T_i,1} & g_{T_i,2} & \cdots & g_{T_i,N_t} \end{bmatrix} \cdot \begin{bmatrix} h_{1,1} & h_{1,2} & \cdots & h_{1,N_r} \\ h_{2,1} & h_{2,2} & \cdots & h_{2,N_r} \\ \vdots & \vdots & \ddots & \vdots \\ h_{N_t,1} & h_{N_t,2} & \cdots & h_{N_t,N_r} \end{bmatrix} + \mathbf{N} \quad (6.3)$$

where g_{t_i,n_t} is the partial spreading sequence (p.s.s.) to be transmitted on antenna n_t and signaling interval t_i. This can be written concisely as:

$$\mathbf{R} = \mathbf{G}_n \mathbf{H}_n + \mathbf{N} \quad (6.4)$$

where $\mathbf{H}_n$ is the channel response for user n and the elements of the noise matrix $\mathbf{N}$ are i.i.d zero mean Gaussian random variables with noise variance N_o. By applying the PDV technique in the space-time decoding sequence (STDS), the decision variable $\mathbf{u}$ is recovered as the received signal multiplied by the desired bit's code subsequences, given by c_{t_i,n_t} for signaling interval t_i and transmit antenna n_t. Therefore for a single user there are $T_i \times N_t$ decision variables for each desired bit b_{l_b} from:

$$\mathbf{U} = \mathbf{C}_{l_b} \mathbf{R} \quad (6.5)$$

where $\mathbf{C}_{l_b}$ is the decoding matrix of the desired bit. This can be written more concisely in terms of each decision p.s.s. at each receive antenna u_{t_i,n_r} and information bit b_{l_b} as:

$$u_{n_t,n_r} = b_{l_b} h_{n_t,n_r} + \sum_{i \neq n_t}^{X} b_i \rho_{i,n_t} h_{i,n_r} + n_o \quad (6.6)$$

where $X = N_t$ and ρ_{i,n_t} is the cross-correlation between the code subsequence of interest n_t and the interfering code subsequence.

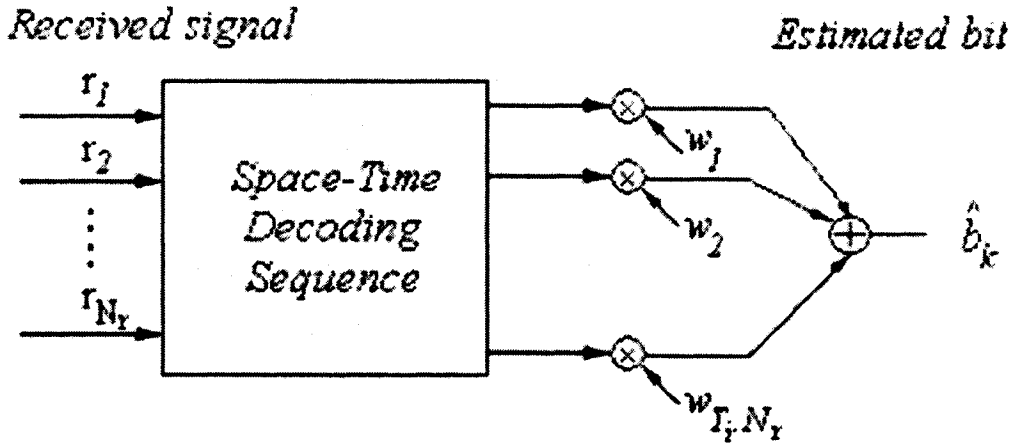

Figure 6.2: Receiving block diagram of the SCDMA system using PDVs.

From the decision variables u_{n_t,n_r}, $n_t = 1,\ldots,N_t$, $n_r = 1,\ldots,N_r$, we can then estimate the l_bth bit as:

$$\hat{\mathbf{b}}_{l_b} = \sum_{n_t=1}^{N_t}\sum_{n_r=1}^{N_r} w^*_{n_t,n_r} u_{n_t,n_r} \tag{6.7}$$

where the weights w_{n_t,n_r} are chosen to maximize the SINR.

To extend this model to include multiple users, we can extend equation (6.6) as:

$$\mathbf{R} = \sum_n \mathbf{G}_n\mathbf{H}_n + \mathbf{N} \tag{6.8}$$

$$\mathbf{U} = \mathbf{C}_{n,l_b}\sum_n \mathbf{G}_n\mathbf{H}_n + \mathbf{N} \tag{6.9}$$

$$= \mathbf{U}_n + \sum_{j\neq n} b_j\boldsymbol{\rho}_{jn}\mathbf{h}_j \tag{6.10}$$

where $\boldsymbol{\rho}_{jn}$ is the cross-correlation vector between the desired user's code partial spreading sequences and all of the interfering users' code partial spreading sequences.

6.4 A Quasi-Orthogonal Coding Block

To design a coding block G, elements of each PDV can be transmitted over any adjacent partial spreading sequence X or transmit antenna. An example of a code block using 4

signaling intervals and 4 transmit antennas to transmit 4 data symbols is shown below:

$$\mathbf{G_1} = \begin{pmatrix} b_1c_1 & b_2c_2 & b_3c_3 & b_4c_4 \\ b_4c_4 & b_1c_1 & b_2c_2 & b_3c_3 \\ b_3c_3 & b_4c_4 & b_1c_1 & b_2c_2 \\ b_2c_2 & b_3c_3 & b_4c_4 & b_1c_1 \end{pmatrix} \tag{6.11}$$

where $b_{i=1,2,3,4}$ is the transmitted data symbols and $c_{j=1,2,3,4}$ is the code subsequence.

The receive vector and the decision vector for bit b_l and user n can now be computed for a N user and $(N_t = N_r = X = 4)$ system as:

$$\mathbf{R} = \sum_n \mathbf{G}_n\mathbf{H}_n + \mathbf{N} \tag{6.12}$$

$$= \sum_n \begin{bmatrix} b_1c_1 & b_2c_2 & b_3c_3 & b_4c_4 \\ b_4c_4 & b_1c_1 & b_2c_2 & b_3c_3 \\ b_3c_3 & b_4c_4 & b_1c_1 & b_2c_2 \\ b_2c_2 & b_3c_3 & b_4c_4 & b_1c_1 \end{bmatrix} \cdot \begin{bmatrix} h_{11} & h_{21} & h_{31} & h_{41} \\ h_{12} & h_{22} & h_{32} & h_{42} \\ h_{13} & h_{23} & h_{33} & h_{43} \\ h_{14} & h_{24} & h_{34} & h_{44} \end{bmatrix} + \mathbf{N} \tag{6.13}$$

$$\mathbf{U} = \mathbf{C}\sum_n \mathbf{G}_n\mathbf{H}_n + \mathbf{N} \tag{6.14}$$

$$= b_1^n h_{11} + \sum_{i\neq 1}^{X} b_i^n \rho_{1i}^n h_{i1}^n + \sum_{j\neq n}^{N}\sum_{i=1}^{X} b_i^j \rho_{1i}^j h_{i1}^j \tag{6.15}$$

where the first term is the desired information bit, the second term is the self MAI caused by the desired users information bits transmitted on different antennas and the third term is the MAI cause by other transmitting users.

For the coding block $\mathbf{G_1}$ we transmit the same SS over different symbol intervals and antenna. If one SS experiences more fading from one antenna than another, this will be compensated at the receiver, where the LMS algorithm will weight each PDV to minimize the MMSE. Using this code we try to maximize spatial, temporal and code diversity.

6.5 Simulation Results

In this section simulations were performed using the same parameters as those discussed in Chapter 4. The coding block from equation (6.11) has been implemented and its performance demonstrated through simulated and measured channel data for 4 transmitting and receiving antennas. The extension of the technique to provide adaptive data rates by varying specific parameters will also be discussed and illustrated with examples.

For our simulations, similar assumptions have been made to those in Chapter 4. Using a quasi-static Rayleigh fading channel where we assumed that the fading coefficients are constant within each trial but vary from trial to trial, we used the following parameters:

1. We are considering a symbol synchronous N user DS-CDMA system employing BPSK modulation;
2. All thermal noise is assumed to be AWGN;
3. All signals are transmitted at the same bit rate;
4. Channels are assumed to be linear;
5. All users are received with equal power gain;
6. Techniques used to find weighting of each p.s.s. and signaling interval will include LMS (described in Chapter 3);
7. The training length used is 2000 bits;
8. Including training sequences we simulated 100 trials with 16000 bits per trial, where every trial we regenerated the channel gain and spreading sequences. The results of all the trials are then averaged to find performance results.

Figure 6.3 presents a 4 user system, each user transmitting with 4 transmit antennas, a spreading sequence of 20 and the receiver having 4 antennas. From the figure the modified PDV technique shows that with the coding block described in (6.11) an improvement in BER performance is seen at a $E_b/N_o \geq$ 5dB compared to using a single partial decision variable (1 PDV).

6.5.1 Adaptive Transmission Rate

An important parameter dealing with transmission is the rate at which information can be sent. In the above simulations we considered 4 users with a spreading factor of 20, giving the system a spectral efficiency of 0.2bps/Hz. However, if we were to decrease the number of time slots from four to three, we have effectively increased the rate of transmission by $\frac{4}{3}$. increasing our original spectral efficiency to 0.267bps/Hz. Figure 6.4 compares different transmission rates by removing rows from the coding block $\mathbf{G}_1$. From the figure as we increase the transmission rate by $\frac{4}{3}$ at an E_b/N_o of 20dB BER decreases by $\frac{1}{2}$ decade. For $E_b/N_o \leq$

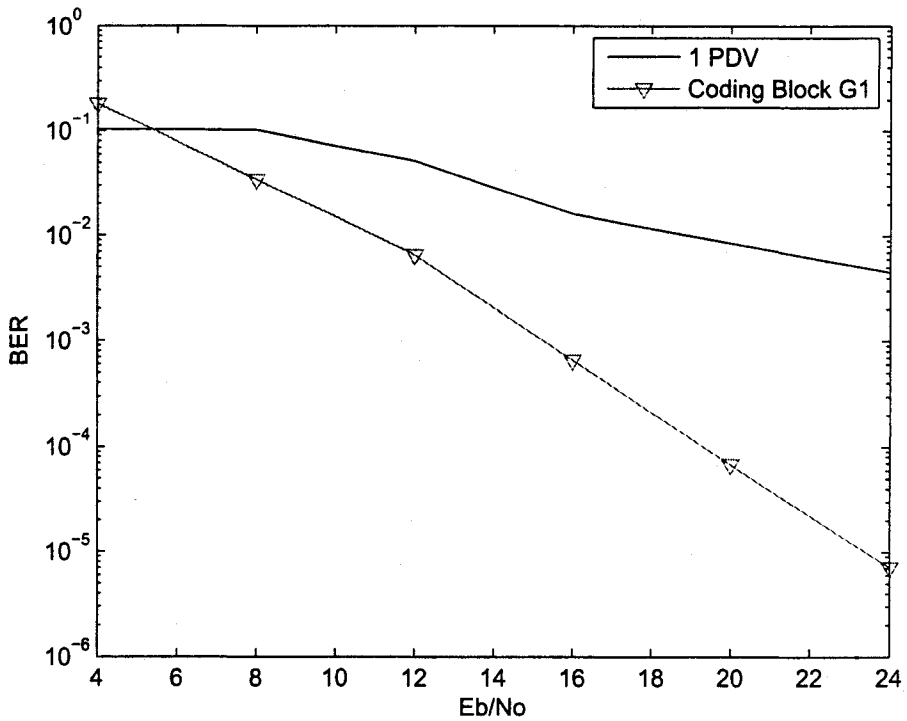

Figure 6.3: Modified PDV with 4 users, $N_t = N_r = 4$, SF = 20 and coding block $\mathbf{G}_1$.

8dB, we see that using a lower transmission rate produced lower BER performance. These errors however are introduced because of the additional LMS weighting used for calculations (which was discussed in Chapter 4). This illustrates the advantages of PDVs: by decreasing the number of signaling intervals and PDVs we can adapt our system to situations where higher transmission rates are necessary with lower E_b/N_o.

Another method used to increase transmission rate of a system is to decrease the spreading factor and use the additional signaling intervals to send information. Figure 6.5 compares the BER performance of 2 different systems with 4 transmit/receiver antennas. The first, is a 4 user system with a spreading factor of 40 transmitting 4 bits over 2 time slots. The second, is a 4 user system with a spreading factor of 20 transmitting 4 bits over 4 time slots. From our simulations both systems are transmitting at the same spectral efficiency, but from the figure, using more time slots achieves a better BER performance. This method shows another advantage of PDVs: by increasing the number of PDVs, we can increase spectral efficiency and BER performance by mitigating interference.

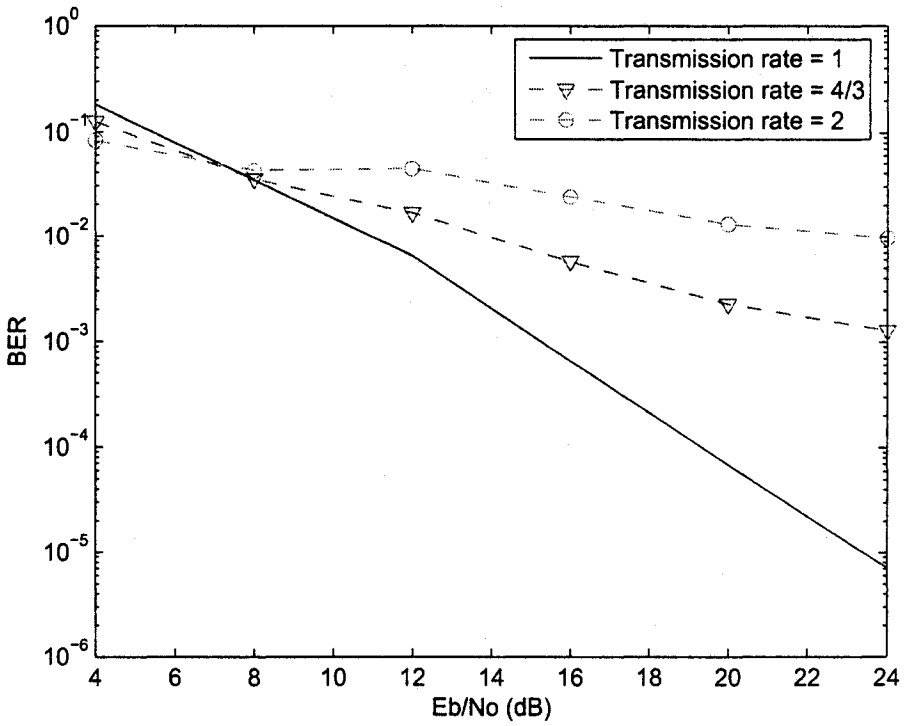

Figure 6.4: SCDMA using PDV technique with 4 users, $N_t = N_r = 4$, SF = 20 and coding block $\mathbf{G}_1$ with varying transmission rate.

6.5.2 Measured Channel Data

In this section, the use of measured channel data will be explored using PDVs for a SCDMA system. In the measurements, the receiver is located within a street in downtown Ottawa. In different intersections copies of the transmitted signal can arrive from different directions, reflected from objects around the intersection, resulting in spatial correlation at the receiver. For our simulations, different measured channels were kept constant over each trial, but varied from trial to trial. Figure 6.6 compares the use of a 4 user, 4 receive/transmit antenna system with a spreading factor of 20 with different transmission rates in measured channel data. From results, using measured channel data decreases BER performance, which is consistent with results obtained in Chapter 4 and slightly lower then in Figure 6.4. However, using a transmission rate of $\frac{4}{3}$ the loss at E_b/N_o = 17dB, decreased from 2 decades in Figure 6.4 to 1 decade in Figure 6.6. This difference can be attributed to the correlations in

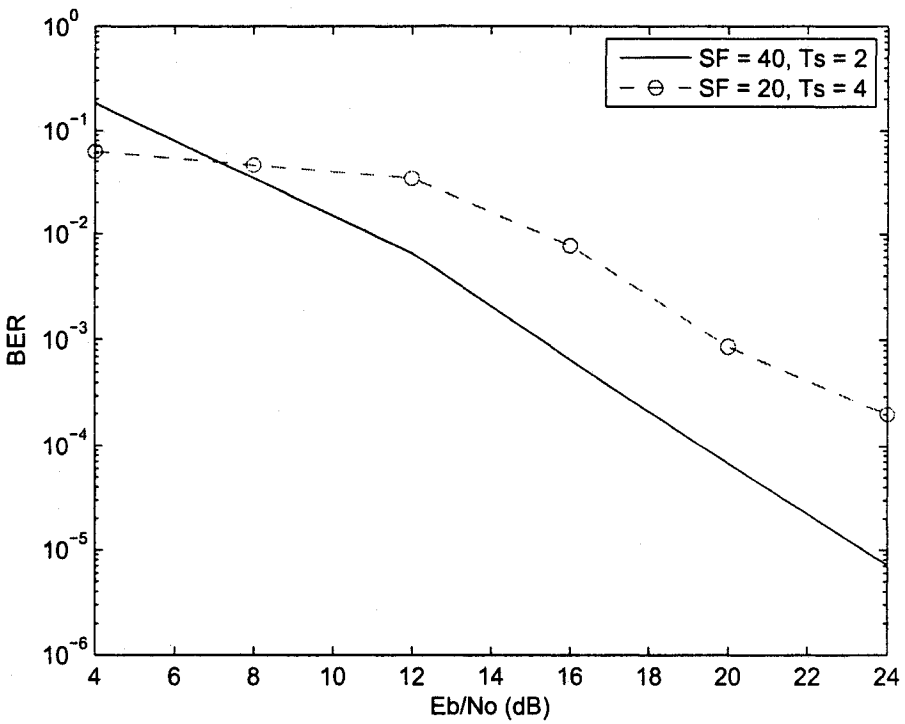

Figure 6.5: SCDMA using PDV technique with 4 users, $N_t = N_r = 4$, with different spreading sequences and a coding block $\mathbf{G}_1$.

the channel, with the addition of PDVs improvements are not as high as those in a simulated channel.

6.6 Summary

In this section we designed a modified PDV technique, employing PDVs for a SCDMA system. In the case of a quasi-static Rayleigh fading channel, results obtained show the PDV technique having significantly better performance than 1 PDVs with multiple receive antennas. This is because the coding block $\mathbf{G}_1$ designed above transmits the same SS over different symbol intervals and antenna. If one SS experiences more fading from one antenna than another, this will be compensated at the receiver, where the LMS algorithm will weight each PDV to minimize the MMSE.

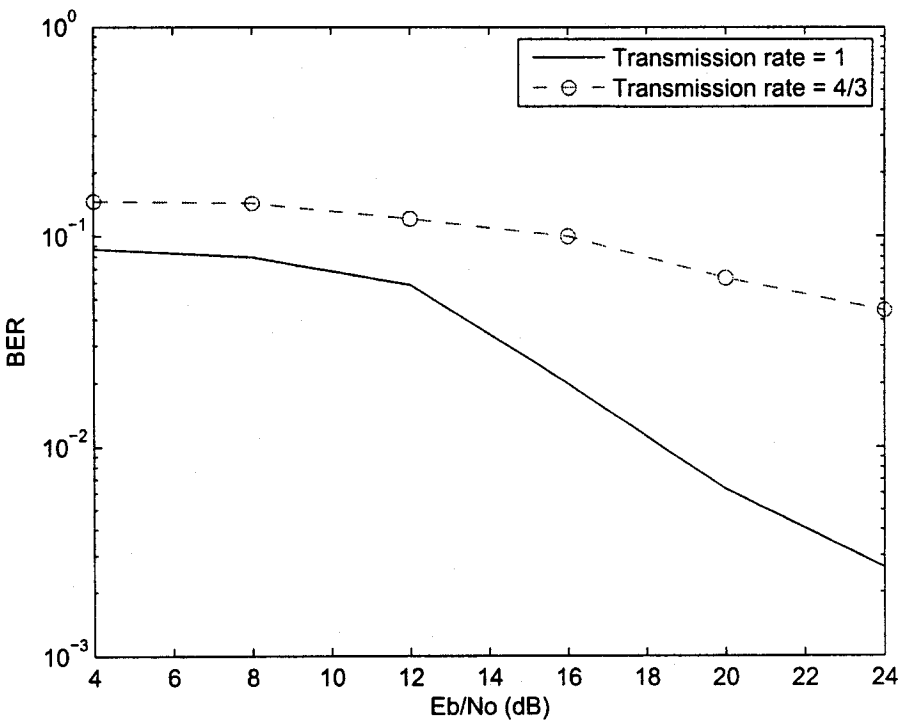

Figure 6.6: SCDMA using PDV technique with 4 users, $N_t = N_r = 4$, SF = 20 with varying transmission rate with measured channel data.

Chapter 7

Conclusions

7.1 Summary

The main purpose of this thesis is to develop and evaluate a low complexity multiuser system that can be easily implemented into existing networks, namely the PDV technique. In this thesis we mainly looked at the PDV technique at the receiver with multiple antennas, but have also included systems with multiple transmit/receive antennas using the modified PDV technique.

From the performance results obtained in Chapter 4 of this thesis the following conclusions can be drawn about PDVs with space diversity at the receiver:

1. With the addition of spatial diversity at the receiver, PDVs provide large BER performances over a single diversity path system;
2. In the case of a slowly varying frequency nonselective Rayleigh fading channel with 6 users, 4 receive antennas, with a spreading sequence of 20 and optimized LMS step sizes, the use of 5 PDVs show promising results for $E_b/N_o \geq$ 16dB. In the case of 2 PDVs, performance gains are less significant but can operate at a $E_b/N_o \geq$ 8dB.
3. When using measured channel data, overall BER performance decrease but gains provided by PDV at lower E_b/N_o is more apparent. When implementing a 4 user, 4 receive antennas system with a spreading sequence of 20 and optimized LMS step sizes, the region in which 5 PDVs outperform not using PDVs is decreased to 12dB.
4. The use of PDVs is dependent on choosing the optimized LMS step size. If a correct step size is not chosen, performance can decrease significantly.

5. Using the PDV technique requires a computational complexity of $5KXN_r+(KXN_r-1)$ which is XK times more than conventional detection.

6. When using PDVs it is important to know what E_b/N_o you are operating in. By choosing a specific number of PDVs given a certain E_b/N_o, we can optimize performance.

From the performance results obtained in Chapter 5 of this thesis the following conclusions can be drawn about PDVs with space diversity at the receiver and transmitter:

1. In the case of a quasi-static Rayleigh fading channel and measured channel with 4 user, 4 transmit/receive antenna system and a spreading factor of 20, using the modified PDV technique shows gains over 1 PDV.

2. By removing a time-slot from the coding matrix we are able to increase transmission rate at cost of BER. For the same system mentioned above, by removing one time-slot from the coding matrix $\mathbf{G}_1$ we can increase the transmission rate by $\frac{4}{3}$ by decreasing E_b/N_o at 17dB by 1 decade.

3. Using specifically designed coding blocks, we can try to maximize spatial, temporal and code diversity. If one signal experiences more fading or cross-correlation than another, the receiver will compensate, where the LMS algorithm will weight each PDV to minimize the MMSE.

7.2 Future Work

The performance of the PDV technique has been thoroughly analyzed throughout this thesis with some extensions. However, there are many other opportunities for further research.

With using LMS to calculate our optimum weights, we found a relatively low complexity MMSE detection technique. The drawback in using this, was the values of μ were dependent on various parameters in the system. Further analysis could develop a general equation that could estimate the value of μ given parameters such as the number of transmitting users, number of receiving antennas, and number of partial decision variables.

For synchronous DS-CDMA with multiple transmit and/or receive antennas, a SCDMA system can be designed. In our simulations we specified 2 distinct code blocks, showing

BER improvements as well as transmission rate improvements over no PDVs methods. Future work to be accomplished in this area can include investigation into different coding blocks, altering its dimensions for optimized performance.

In [20] real channel data was presented and analyzed for the downtown core of Ottawa. Results showed that in different areas correlation and diversity varied significantly. In our simulations only a small set of data we used. Further data can be obtained from these trials and used in analyzing PDVs in different channel conditions (i.e. highly correlated environments). This will provide us with invaluable information on the practical implementation of this technique.

Bibliography

[1] T. Rappaport, *Wireless Communications: Principles and Practice.* New Jersey: Prentice Hall, 1996.

[2] A. J. Viterbi, "When not to spread spectrum - a sequel," *IEEE Commun. Mag.*, vol. 23, pp. 12–17, Apr. 1985.

[3] C. D'Amours, R. El-Abdallah, and S. Nathoo, "A simple multi-user detector employing adaptive filters," in *Proc. CCECE 2003 - Canadian Conference on Electrical and Computer Engineering*, (Ottawa, ON), pp. 1675–1678, May 2003.

[4] S. Moshavvi, "Multi-user detection for DS-CDMA communications," *IEEE Commun. Mag.*, vol. 34, pp. 124–136, Oct. 1996.

[5] S. Verdú, "Minimum probability of error for asynchronous Gaussian multiple-access channels," *IEEE Trans. Inform. Theory*, vol. 32, pp. 85–96, Jan. 1986.

[6] S. Verdu, *Multiuser Detection.* United Kingdom: Cambridge University Press, 1998.

[7] R. Lupas and S. Verdu, "Linear multiuser detectors for synchronous code-division multiple-access channel," *IEEE Trans. Inform. Theory*, vol. 35, pp. 123–136, Jan. 1989.

[8] M. Honig, U. Madhow, and S. Verdu, "Blind adaptive multiuser detection," *IEEE Trans. Inform. Theory*, vol. 41, pp. 944–960, July 1995.

[9] A. Duel-Hallen, "A family of multiuser decision-feedback detectors for asynchronous code-division multiple access channels," *IEEE Trans. Commun.*, vol. 43, pp. 421–434, Feb. 1995.

[10] M. Varanasi and B. Aahang, "Multistage detection in asynchronous codedivision multiple-access communications," *IEEE Trans. Commun.*, vol. 38, pp. 509–519, Apr. 1990.

[11] A. Duel-Hallen, "Decorrelating decision-feedback multiuser detector for synchronous code-division multiple-access channel," *IEEE Trans. Commun.*, vol. 41, pp. 285–290, Feb. 1993.

[12] A. Duel-Hallen, "On suboptimal detection for asynchronous code-division multiple access channels," in *Proc. ISS 1992 - 26th Annual Conference on Information Sciences and Systems*, (Princeton, NJ), pp. 838–843, Mar. 1992.

[13] G. Stewart, *Introduction to Matrix Computations.* New York: Academic Press, 1974.

[14] D. Brennan, "Linear diversity combining techniques," *Proc. IRE*, vol. 47, pp. 1075–1102, Feb. 1959.

[15] S. Miller, *Detection and estimation in multiple access channels.* PhD thesis, Princeton University, Princeton, New Jersey, 1989.

[16] R. Kohno, H. Imai, M. Hatori, and S. Pasupathy, "Combination of an adaptive antenna array and a canceler of interference for direct sequence spread spectrum multiple-access system," *IEEE Trans. Commun.*, vol. 8, pp. 675–682, May 1990.

[17] Y. Cho and J. Lee, "Adaptive interference cancellation with diversity combining for a DS-CDMA system in Rayleigh fading," in *Proc. VTC 1999 Spring - IEEE 49th Vehicular Technology Conf.*, (Seoul, Korea), pp. 1899–1902, May 1999.

[18] J. H. Horng and Y.-P. Nakache, "Adaptive diversity combining for interference cancellation in CDMA systems," in *Proc. VTC 2001 Fall - IEEE 54th Vehicular Technology Conf.*, (Murray Hill, NJ), Oct. 2001.

[19] L. Yuan and Q. Zheng, "Blind adaptive distributed decorrelating detector for DS-CDMA systems," in *Proc. TENCON 2002 - Proc. IEEE Region 10 Conf. on Computers, Comm., Control and Power Eng.*, vol. 2, pp. 1064–1068, Aug. 2002.

[20] G. Downes, T. Willink, and C. D'Amours, "Capacity limitations of real MIMO channels and their impact on system performance," in *Proc. WIRELESS 2004 - Proc. 18th Int. Conf. on Wireless Commun.*, (Calgary, Alberta, Canada), pp. 100–104, July 2005.

[21] V. Tarokh, N. Seshadri, and A. R. Calderbank, "Space-time codes for high data rate wireless communication: Performance criterion and code construction," *IEEE Trans. Inform. Theory*, vol. 44, pp. 744–765, Mar. 1998.

[22] G. Foschini, "Layered space-time architecture for wireless communication in a fading environment when using multiple antennas," *Bell Lab. Tech. J.*, vol. 1, pp. 41–59, Sept. 1996.

[23] Z. Zhang, G. Li, and J. Zhu, "A novel decoding algorithm of STBC for CDMA receiver in multipath fading environments," in *Proc. VTC 2001 Fall - IEEE 54th Vehicular Technology Conf.*, pp. 1956–1959, Oct. 2001.

[24] Y. Kou, W. Lu, and A. Antoniou, "Application of space-time block coding in DS-CDMA communication systems," in *Computers and Signal Processing, 2001. PACRIM. 2001 IEEE Pacific Rim Conference on Communications*, (Victoria, BC), pp. 132–135, Aug. 2001.

[25] H. M. Kang and S. H. Cho, "Space-time SIC multiuser detection algorithm and its performance in Rayleigh fading channel," in *IEEE TENCON 2003*, (Bangalore, India), pp. 126–130, Oct. 2003.

[26] Z. Zhang, G. Li, and J. Zhu, "A new SIC algorithm for STBC coded DS-CDMA systems," in *IEEE 6th CAS Symp. on Emerging Technologies: Mobile and Wireless Comm.*, (Shanghai, China), pp. 357–360, May 2004.

[27] W. Choi and J. Andrews, "On spatial multiplexing in cellular MIMO-CDMA systems with linear receivers," in *IEEE International Conference on Communications, 2005*, (Austin, Texas), pp. 2277–2281, May 2005.

[28] D. Reynolds and X. Wang, "Blind adaptive space-time multiuser detection with multiple transmitter and receiver antennas," *IEEE Trans. Signal Processing*, vol. 50, pp. 1261–1276, June 2002.

[29] J. Yang, "A simple transmit diversity scheme for wireless communications," *IEEE Trans. Commun.*, vol. 16, pp. 1451–1458, Oct. 1998.

[30] H. Huang, H. Viswanathan, and G. J. Foschini, "Multiple antennas in cellular CDMA systems: transmission, detection, and spectral efficiency," *IEEE Trans. Wireless Commun.*, vol. 1, pp. 383–392, July 2002.

[31] J. J. Ossana, "A model for mobile radio fading due to building reflections: theoretical and experimental fading waveform power spectra," *Bell Systems Technical Journal,*, vol. 24, pp. 2935–2971, Nov. 1964.

[32] R. H. Clarke, "A statistical theory of mobile-radio reception," *Bell Systems Technical Journal,*, vol. 47, pp. 871–889, June 1968.

[33] M. Gans, "A power spectral theory of propagation in the mobile radio environment," *IEEE Trans. Veh. Technol.*, vol. 21, pp. 27–38, Feb. 1972.

[34] J. Smith, "A computer generated multipath fading simulation for mobile radio," *IEEE Trans. Veh. Technol.*, vol. 24, pp. 39–40, Aug. 1975.

[35] C. Squires, T. Willink, and B. Gagnon, "A flexible platform for MIMO channel characterization and system evaluation," in *Proc. WIRELESS 2003 - Proc. 16th Int. Conf. on Wireless Commun.*, (Calgary, Alberta), July 2003.

[36] J. Proakis, *Digital Communications.* New York, NY: McGraw-Hill, 1995.

[37] T. Jiann-Ann and B. Woerner, "Performance of diversity combining for uniform circular arrays," in *Proc. VTC 2001 Fall - IEEE 54th Vehicular Technology Conf.*, (Blacksburg, VA), pp. 1630–1634, Oct. 2001.

[38] J. Lempiainen and J. Laiho-Steffens, "The performance of polarization diversity schemes at a base station in small/micro cells at 1800 MHz," *Proc. VTC 1998 Fall - IEEE 48th Vehicular Technology Conf.*, vol. 47, pp. 1087–1092, Aug. 1998.

[39] N.Serinken, M. Jorgenson, K. Moreland, S. Chow, and T. Willink, "Polarisation diversity in high frequency radio data systems," *Elect. Lett.*, vol. 32, pp. 1824–1826, Sept. 1996.

[40] W. Jakes, "A comparision of specific space diversity techniques for reduction of fast fading in UHF mobile radio systems," *IEEE Trans. Veh. Technol.*, vol. VT-20, pp. 87–93, Nov. 1971.

[41] C. Squires, G. Colman, and T. Willink, "A performance comparison of diversity strategies for interference and jamming mitigation," in *Proc. WIRELESS 2004 - Proc. 18th Int. Conf. on Wireless Commun.*, (Calgary, Alberta, Canada), July 2005.

[42] S. Haykin, *Adaptive Filter Theory.* Upper Saddle River, New Jersey: Prentice-Hall, 1996.

[43] B. Widrow, P. Mantey, L. Griffiths, and B. Goode, "Adaptive antenna systems," *Proceedings of the IEEE*, vol. 55, pp. 2143–2159, Dec. 1967.

[44] V. Solo and X. Kong, *Adaptive Signal Procssing Algorithms: Stability and Performance.* Baltimore, MD: Prentice-Hall, 1995.

[45] G. Colman, "A comparison of gradient and block adaptive array algorithm performance in different environments," in *Proc. IST-039/RSY-012 Joint SET/IST Symposium (Chester,UK)*, (Chester,UK), Apr. 2003.

[46] B. V. Veen and K. Buckley, "Beamforming: A versatile approach to spatial filtering," *IEEE ASSP Magazine*, vol. 5, pp. 2–24, Apr. 1988.

[47] J. Cavers, "An analysis of pilot symbol assisted modulation for Rayleigh fading channels (mobile radio)," *IEEE Trans. Veh. Technol.*, vol. 40, pp. 686–693, Nov. 1991.

[48] K. Yu and I. B. Collings, "Pilot symbol aided adaptive receiver for Rayleigh faded CDMA channels," *Proc. Globecom 2001 - IEEE Global Telecommunications Conf.*, vol. 6, pp. 29–40, Jan. 1995.

[49] J. S. Evans, "Optimal resources allocation for pilot symbol aided multiuser receivers in Rayleigh faded CDMA channels," *IEEE Trans. Commun.*, vol. 50, pp. 1316–1325, Aug. 2002.

[50] C. D'Amours, "A reduced-complexity multistage detection algorithm for DS-CDMA systems in AWGN channels," *Canadian Journal of Electrical and Computer Engineering,*, vol. 28, pp. 131–137, June 2003.

[51] V. Tarokh, H. Jafarkhani, and A. R. Calderbank, "Space-time block coding for wireless communications: performance results," *IEEE J. Select. Areas Commun.*, vol. 17, pp. 451–460, Mar. 1999.

[52] V. Tarokh, H. Jafarkhani, and A. R. Calderbank, "Space-time block coding for wireless communications: performance results," *IEEE Trans. Inform. Theory*, vol. 45, pp. 1456–1467, July 1999.